Investigtion of Magnetoelectric Correlations with Nonlinear Optics

- Nonlinear Optics and Symmetry
- Cr_2O_3 as Case Study
- Experimental Setup
- Magnetoelectric effects in multiferroic $RMnO_3$
- Summary

M. Fiebig, (HISKP, Universität Bonn)

Oberseminar Cologne/Bonn, 11.06.2007

universitätbonn

Magnetoelectric Correlations in Multiferroics

- **Nonlinear Optics and Symmetry**
- **Cr_2O_3 as Case Study**
- **Experimental Setup**
- **Magnetoelectric Effects in Multiferroic $RMnO_3$**
- **Summary**

Idea of the Magnetoelectric Effect

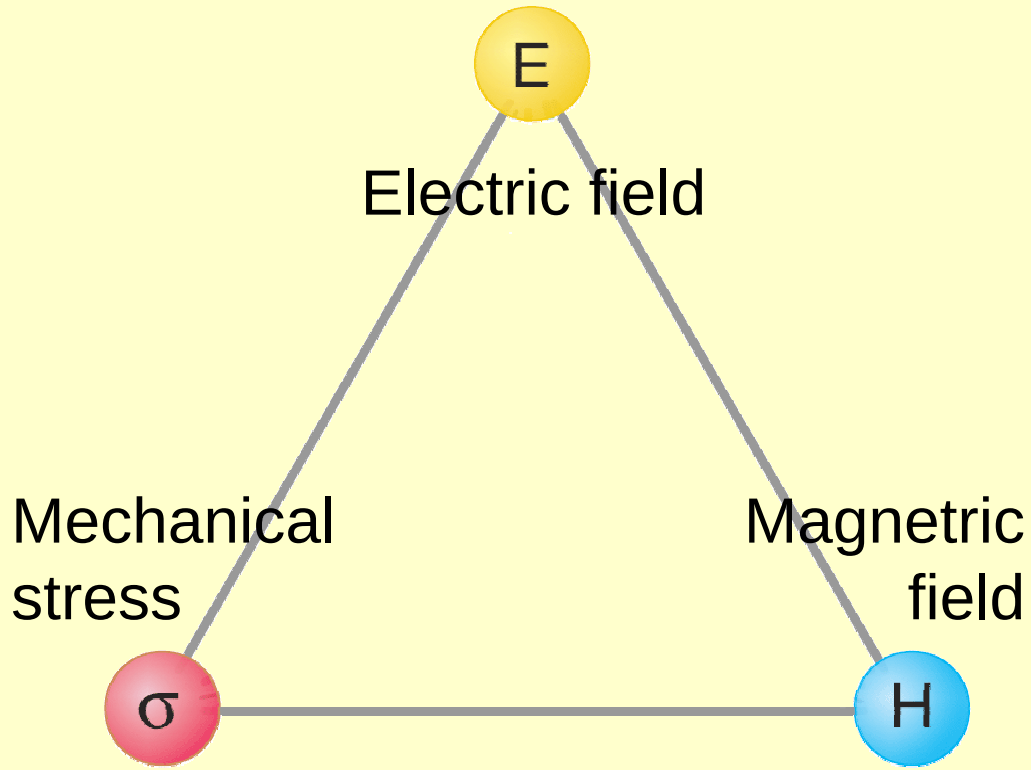

Idea of the Magnetoelectric Effect

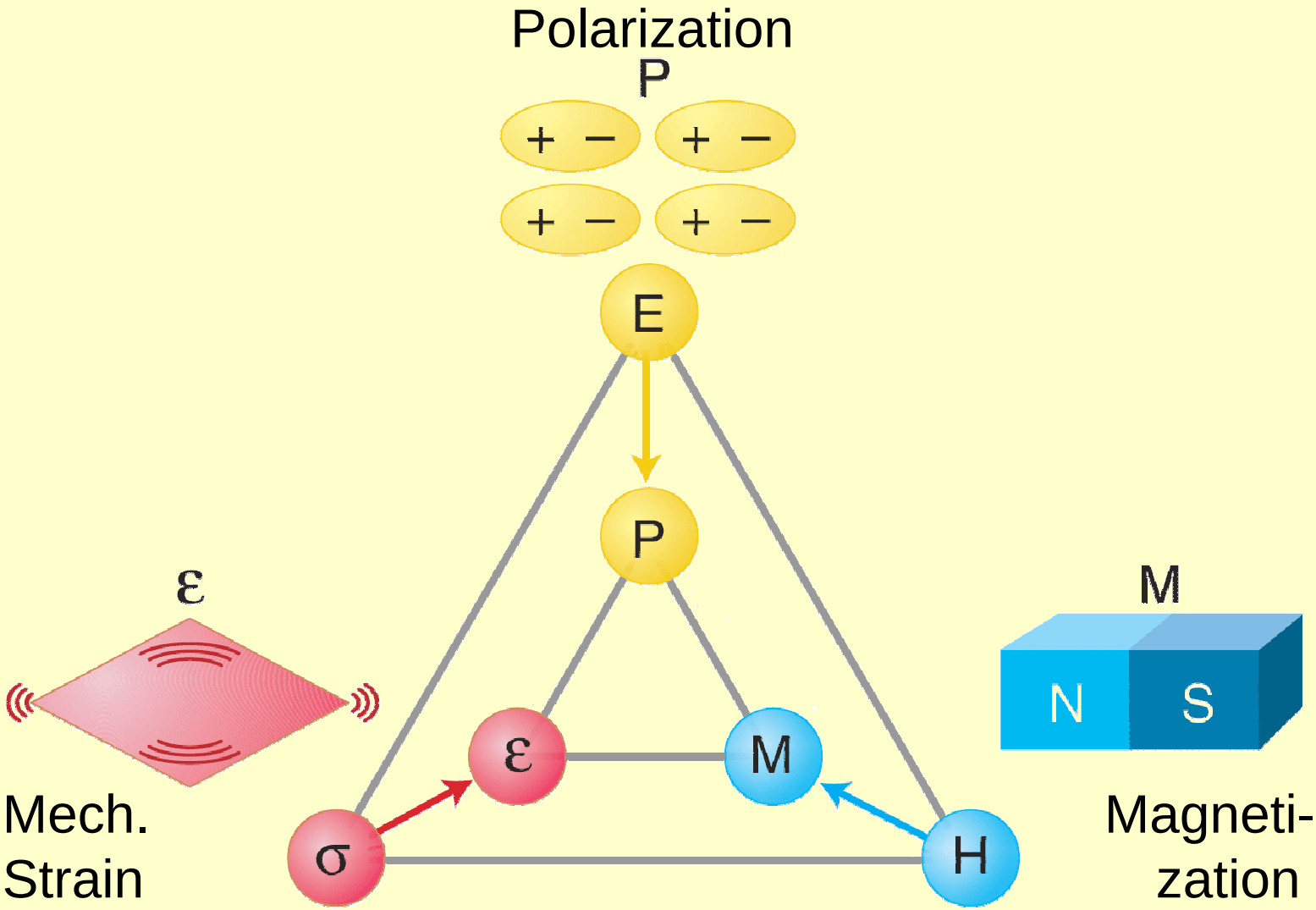

Idea of the Magnetoelectric Effect

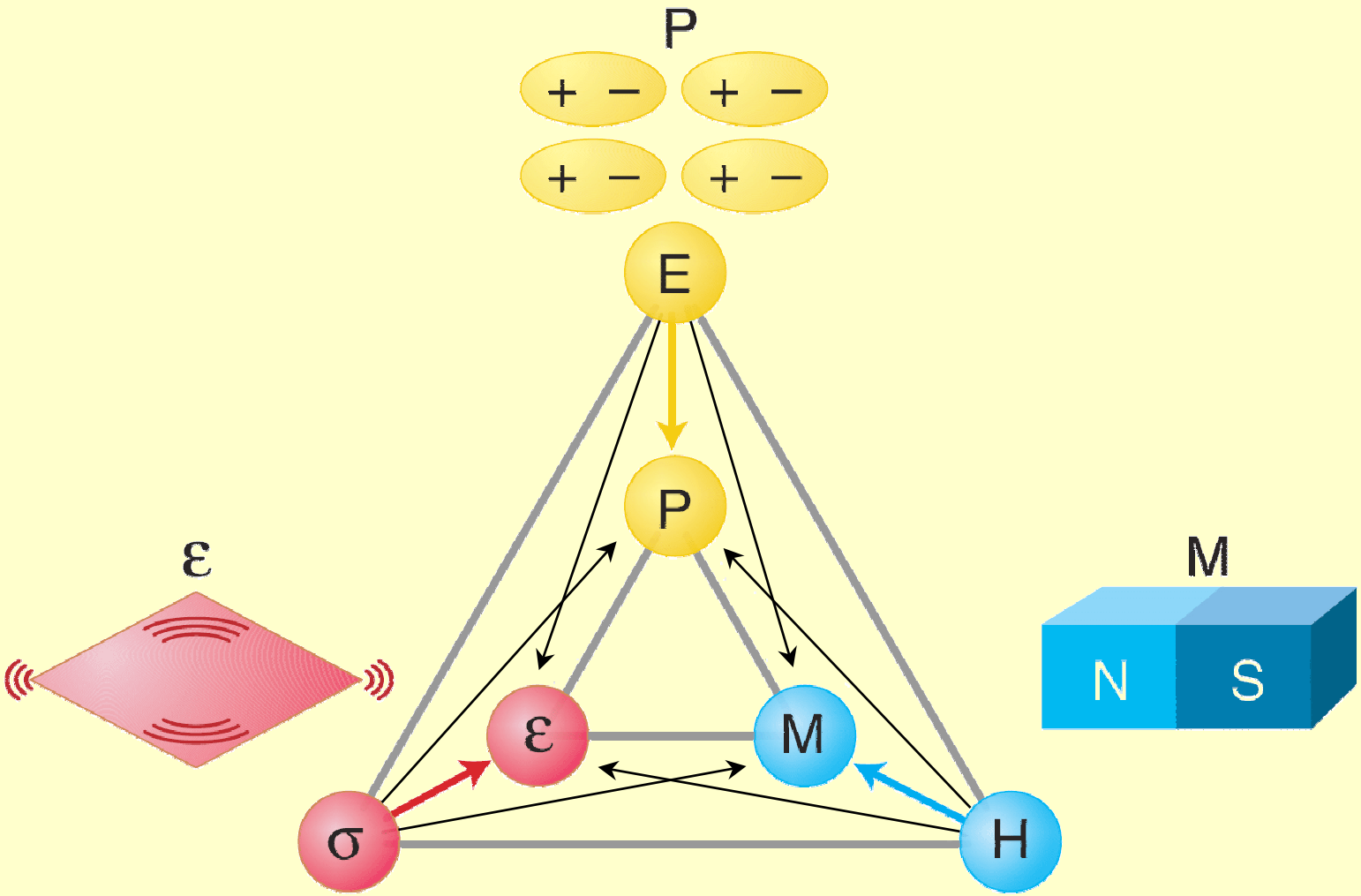

Idea of the Magnetoelectric Effect

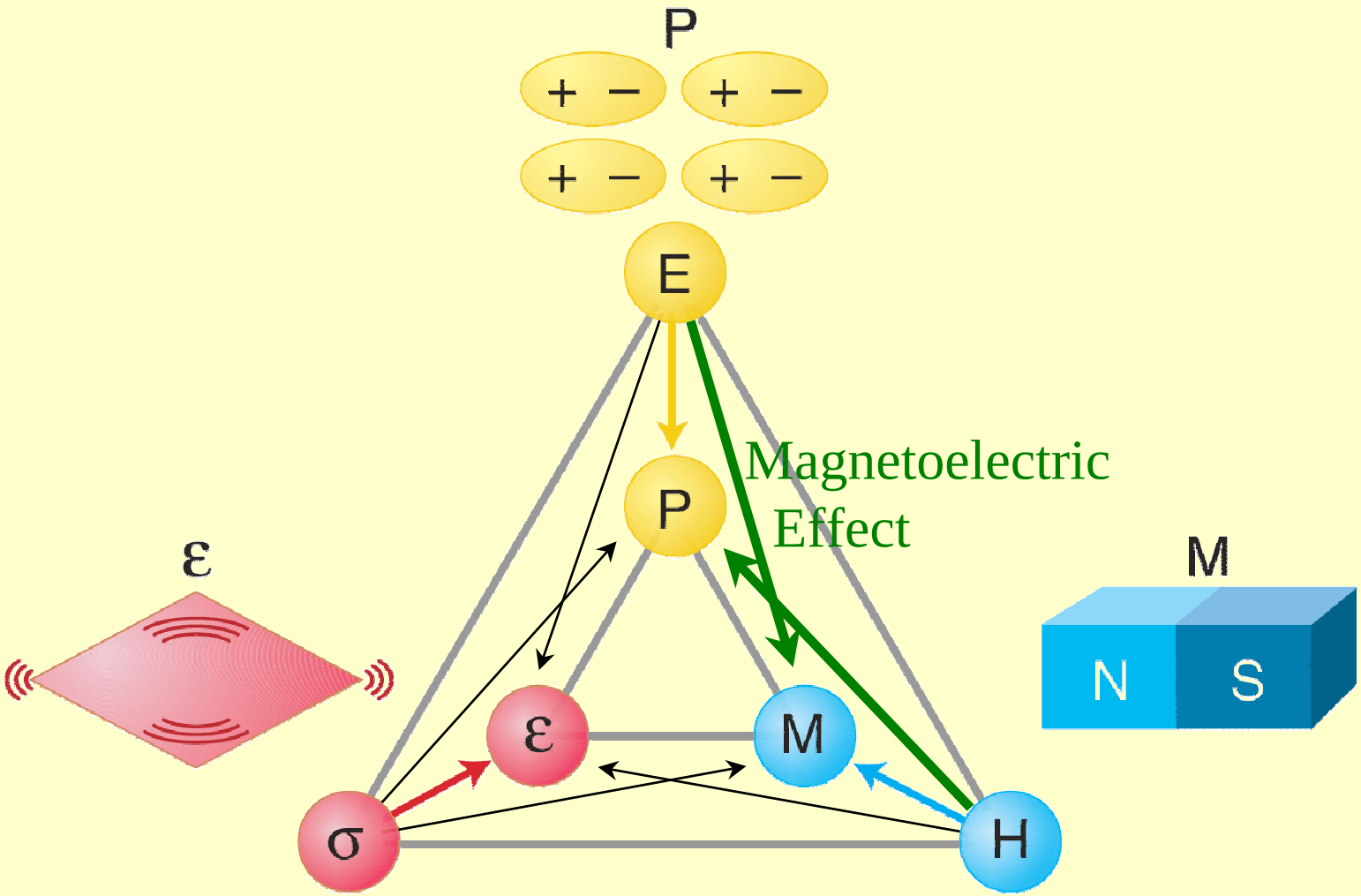

Large Magnetoelectric Effects in Multiferroics

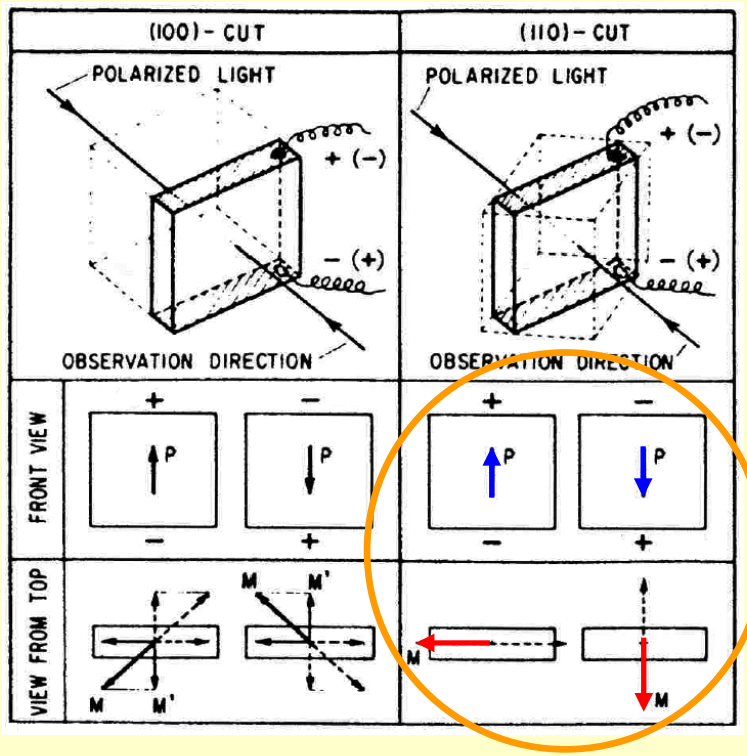

E. Ascher, H. Schmid et al., J. Appl. Phys. **37**, 1404 (1966)

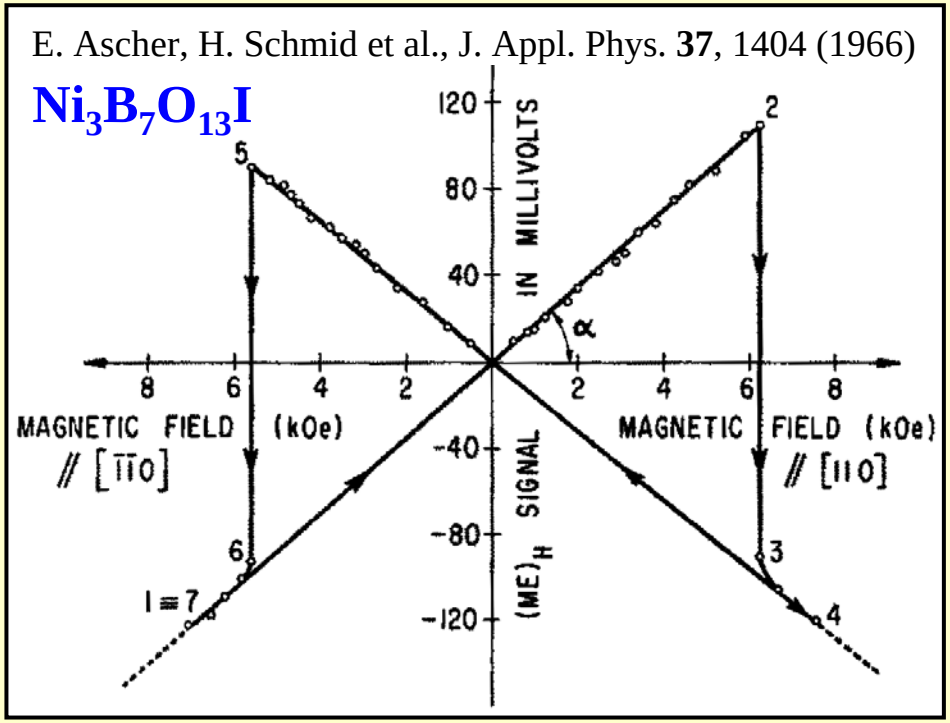

- Rotation of magnetization by 90° [1̲10] → [1̲10]
- Triggers reversal of ferroelectric polarization [001] → [001̲]
- First example of magnetoelectric cross-control

Access to the Magnetoelectric Coupling?

What do we want to investigate?

- Magnetic Structure
- Electric Structure
- Magnetoelectric interaction between magnetic and electric state

What is needed for the investigation?

- Single technique for accessing magnetic and electric structure
- Ferroic order $\leftrightarrow$ domains! Need to see them (spatial resolution)

What is a common property of magnetic and electric structures allowing simultaneous access to both with the same technique?

Symmetry!

Long-Range Order and Symmetry

Long - range ordering | Space inversion | Time reversal

Magnetic

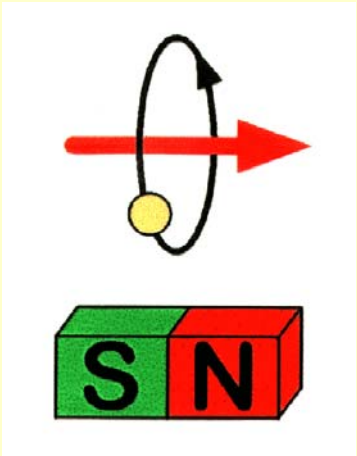

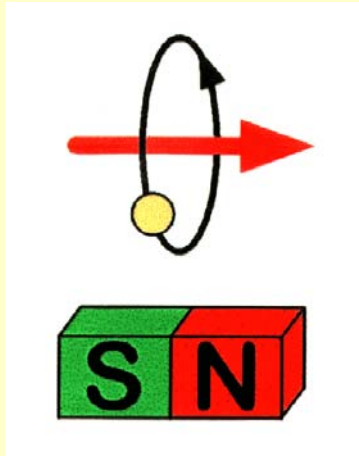

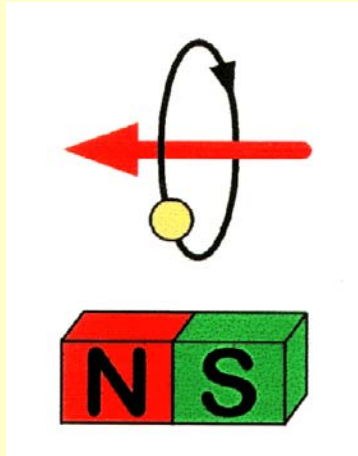

Electric

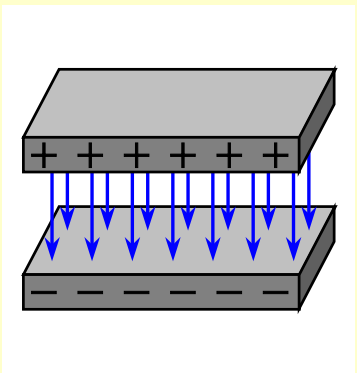

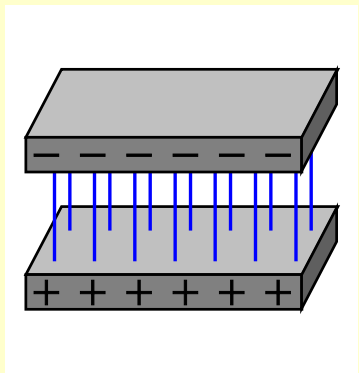

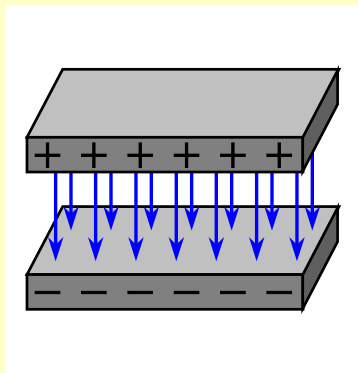

- Violation of symmetry by magnetic as well as electric ordering
- Expect novel effects coupling to the symmetry reduction

Reduction of Symmetry by Magnetic Ordering

Without magnetic order

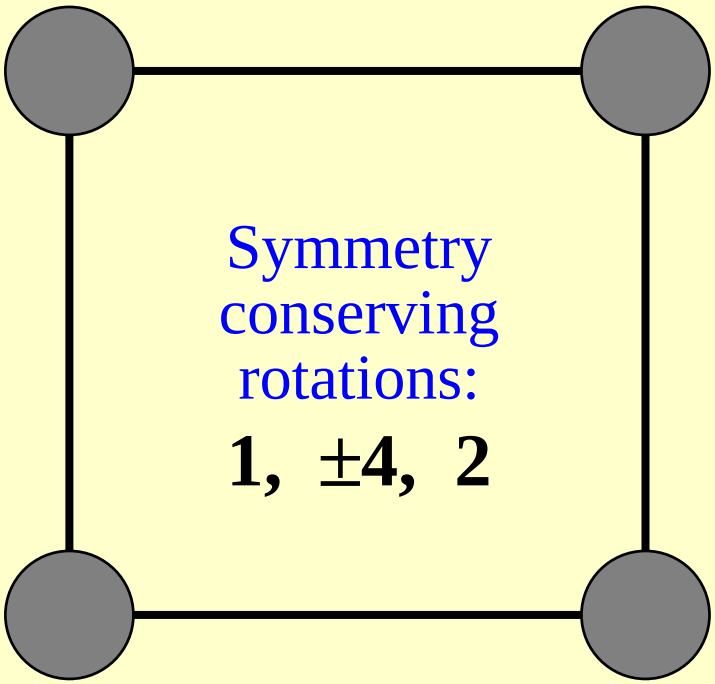

With antiferromagnetism

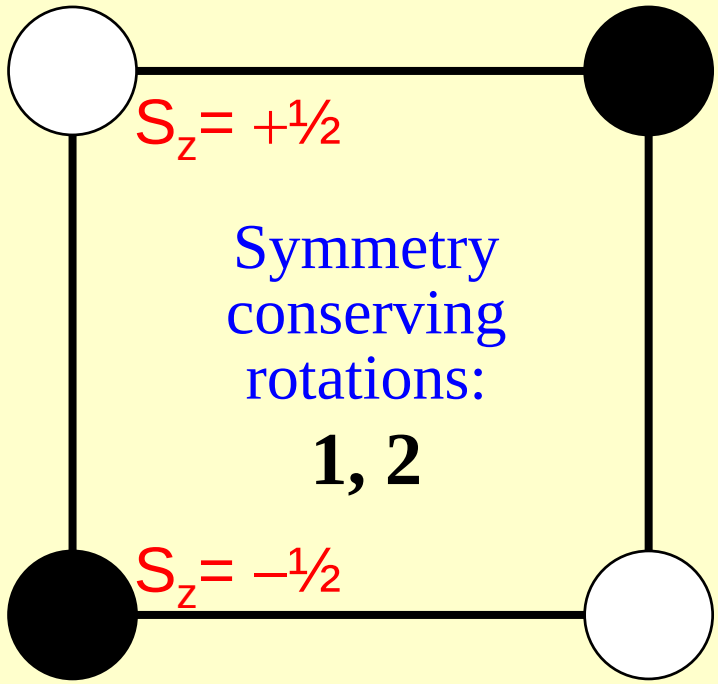

Reduction of symmetry:

- Expect novel effects, induced by the magnetic breaking of symmetry
- Employ these effects as probe for the magnetic order!

Access to the Magnetoelectric Coupling?

What do we want to investigate?

- Magnetic Structure
- Electric Structure
- Magnetoelectric interaction between magnetic and electric state

What is needed for the investigation?

- Single technique for accessing magnetic and electric structure
- Ferroic order ↔ domains! Need to see them (spatial resolution)

What is a common property of magnetic and electric structures allowing simultaneous access to both with the same technique?

Symmetry!

Optical techniques!

Nonlinear Optics

Electric field in matter:

$P(\omega) = \varepsilon_0 \chi\, E(\omega) \sim e^{i\omega t}$

Linear approximation only for weak (light) fields

For strong electromagnetic fields (e.g. laser):

$P = \varepsilon_0 (\chi^{(1)} E + \chi^{(2)} E\, E + \chi^{(3)} E\, E\, E + \ldots)$

With leading-order nonlinear term:

$P(2\omega) = \varepsilon_0 \chi^{(2)} E(\omega)\, E(\omega) \sim e^{i2\omega t}$

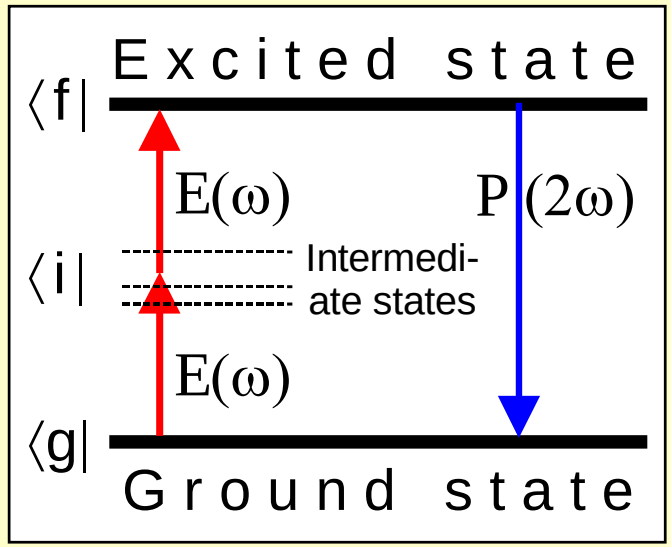

→ **Frequency doubling** ("second harmonic generation", SHG)

$$\chi^{(2)} \propto \sum_i \frac{\langle g | e\vec{r} | f \rangle \langle f | e\vec{r} | i \rangle \langle i | e\vec{r} | g \rangle}{(E_f - E_g - 2\hbar\omega)(E_i - E_g - \hbar\omega)}$$

Microscopically:
second-order perturbation

In general:
resonant

In general:
non-resonant

States ⟨ i | are real states that are excited with large energy mismatch: $\Delta E \cdot \Delta t \sim \hbar$

First Observation of Optical SHG

VOLUME 7, NUMBER 4 PHYSICAL REVIEW LETTERS AUGUST 15, 1961

GENERATION OF OPTICAL HARMONICS*

P. A. Franken, A. E. Hill, C. W. Peters, and G. Weinreich
The Harrison M. Randall Laboratory of Physics, The University of Michigan, Ann Arbor, Michigan

(Received July 21, 1961)

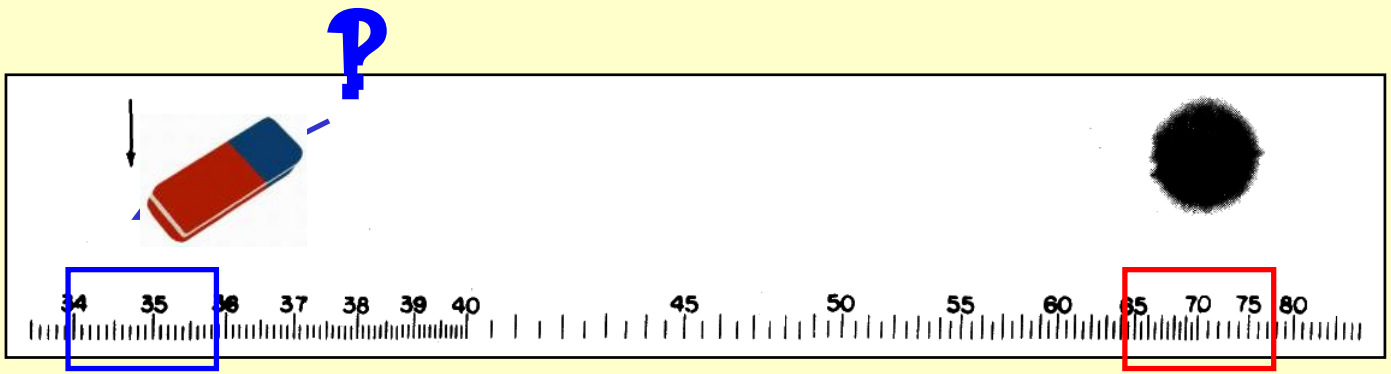

SHG in Multiferroic Compounds

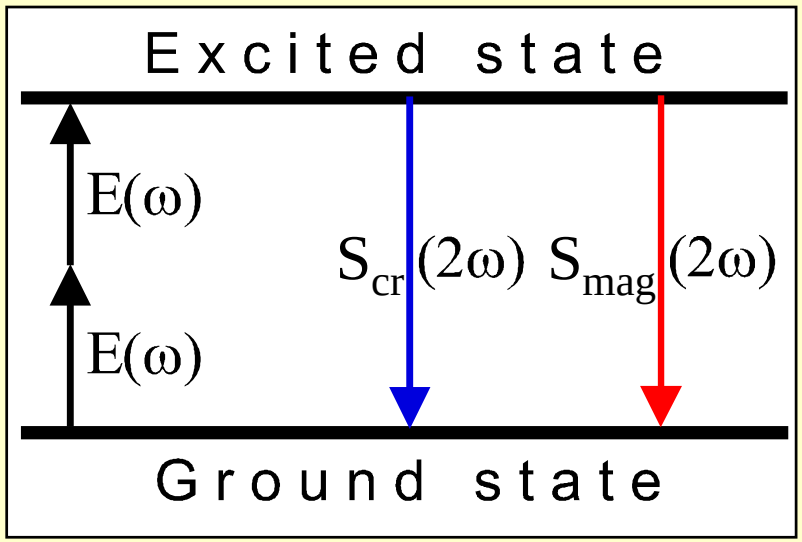

Incident laser beam

Nonlinear signal:

electrical magnetic

Interference !

SHG: $S_i(2\omega) \propto \chi_{ijk} E_j(\omega) E_k(\omega)$

- Only based on symmetry arguments: $\chi_{ijk} \leftrightarrow$ symmetry $\leftrightarrow$ structure
- Access to magnetic *and* electrical structure with the *same* technique

Optical degrees of freedom:

- Spectroscopy: Excitation and emitted signal are sublattice selective
- Spatial resolution: imaging of domain structures, inhomogeneities
- Temporal resolution: dynamics down to sub-picosecond range

Nonlinear optics reveals novel information about magnetic and electrical structure

Magnetic Ordering and Symmetry

Nonlinear optical susceptibility of magnetically ordered crystals

N. N. Akhmediev, S. B. Borisov, A. K. Zvezdin, I. L. Lyubchanskiĭ, and Yu. V. Melikhov

Physicotechnical Institute, Academy of Sciences of the Ukrainian SSR, Donetsk

(Submitted September 24, 1984)

Fiz. Tverd. Tela (Leningrad) **27**, 1075–1078 (April 1985) Sov. Phys. Solid State **27**(4), 650, April 1985

Group-theoretic analysis is given of the nonlinear optical susceptibility of magnetic materials due to their magnetic ordering and due to an applied magnetic field. Rare-earth orthoferrites are considered as an example.

"When the effects related to magnetic ordering and the presence of an applied magnetic field are studied, it is necessary to take account of the fact that the **symmetry of the magnetic subsystem can be lower than the symmetry of the crystal lattice**."

First Magnetic SHG Experiment

VOLUME 67, NUMBER 20 PHYSICAL REVIEW LETTERS 11 NOVEMBER 1991

Effects of Surface Magnetism on Optical Second Harmonic Generation

J. Reif, J. C. Zink, C.-M. Schneider, and J. Kirschner

Institut für Experimentalphysik, Freie Universität Berlin, Arnimallee 14, W-1000 Berlin 33, Germany

(Received 21 May 1991)

We report on the first experiments showing the influence of surface magnetization on optical second harmonic generation in reflection at a Fe(110) surface. The magneto-optical Kerr effect modifies the hyperpolarizability of the surface in the optical field, leading to a dependence of the second harmonic yield on the direction of magnetization relative to the light fields. For the clean surface an effect of 25% was determined, which decays exponentially with surface contamination by the residual gas, thus demonstrating the high surface sensitivity of this technique.

2878

PACS numbers: 75.30.Pd, 78.20.Ls, 78.65.Ez

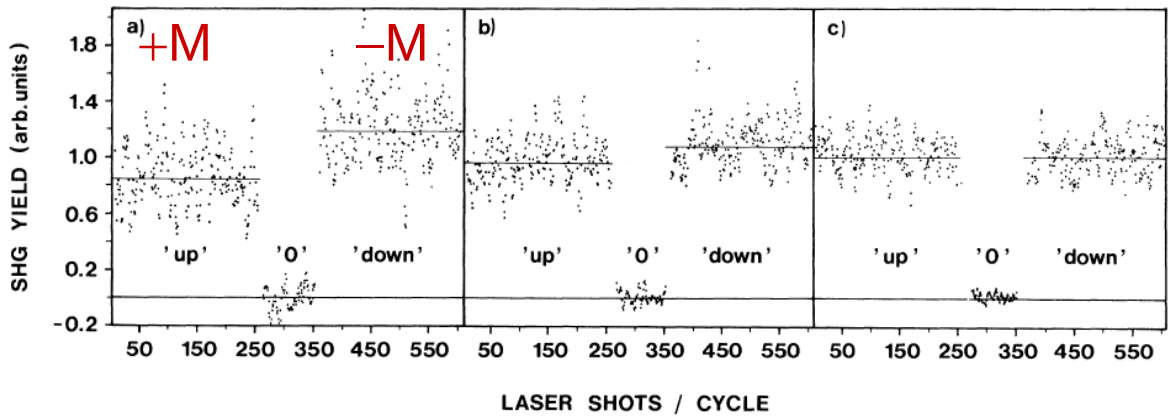

FIG. 2. Relative magnetization dependence of second harmonic signal for three different times elapsed since sample preparation [(a) ≈ 45 min, (b) ≈ 60 min, (c) ≥ 180 min]. Shown is, in each panel, an averaged [superposition of (a) 220, (b) 550, and (c) 750 cycles] experimental cycle, consisting of 250 pulses with magnetization "up," 100 pulses with no SHG signal (obtained by means of a UV blocking glass filter), and 250 pulses with magnetization "down." All signals are normalized to the expected value without influence of magnetization [cf. Eq. (1)]. The solid lines represent the average of the respective regions of interest.

Observation of a second harmonic contribution which depends on the magnetization of a Fe(001) surface

Small signal, but with high contrast → typical for SHG!

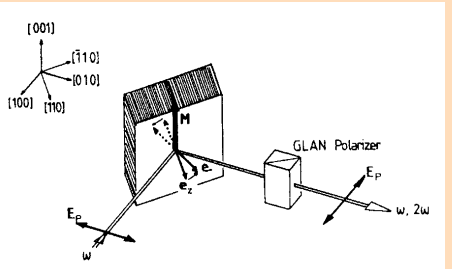

Linear Magneto-Optical Effects

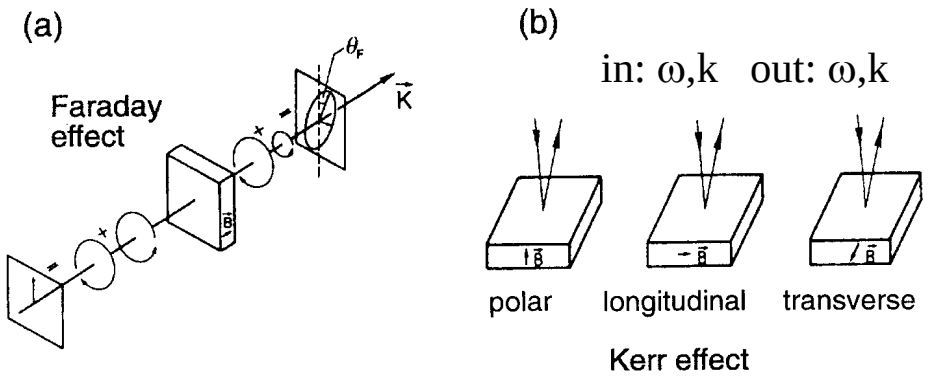

Dielectric function :

$$\tilde{\varepsilon} = \varepsilon \begin{pmatrix} 1 & iQ & 0 \\ -iQ & 1 & 0 \\ 0 & 0 & 1 \end{pmatrix}$$

- Rotation of plane of polarization upon transmission/reflection on magnetized medium
- Described by non-diagonal elements of 3×3 matrix
- Q << 1 ⇒ **small effect (10^{-2}...10^{-5})**

Kerr rotation and ellipticity

$$\Phi_{Ks} = \Phi'_{Ks} + i\Phi''_{Ks} = \frac{E_p^{(r)}}{E_s^{(r)}}$$

$$\Phi_{Kp} = \Phi'_{Kp} + i\Phi''_{Kp} = \frac{E_s^{(r)}}{E_p^{(r)}}$$

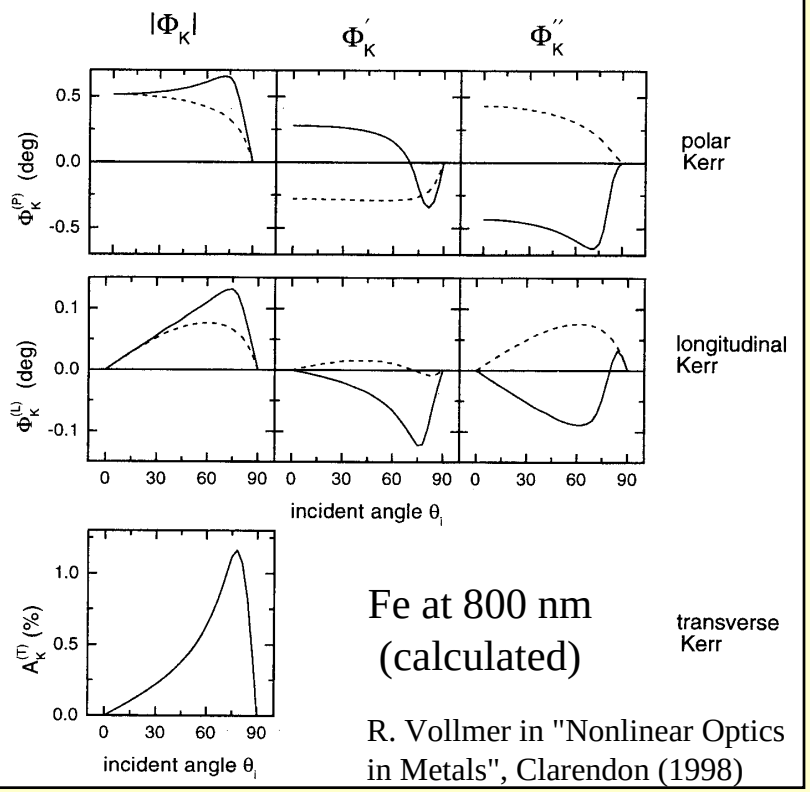

Fe at 800 nm (calculated)

R. Vollmer in "Nonlinear Optics in Metals", Clarendon (1998)

Nonlinear Magneto-Optical Effects

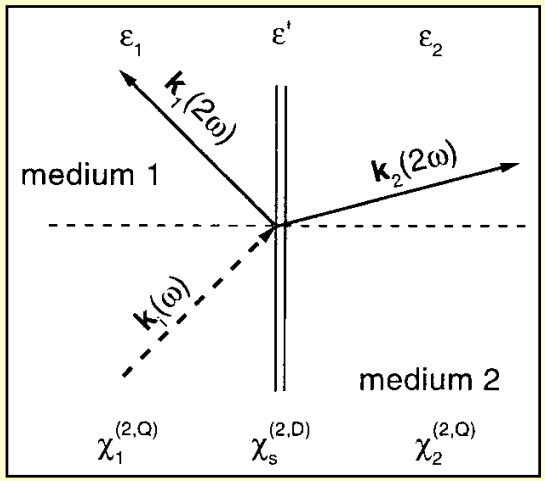

Generation of reflected SH wave:

$$P_i(2\omega) = \chi^{(2)}_{ijk}(M)\, E_j(\omega)\, E_k(\omega)$$

with $\chi^{(2)}(-M) = -\chi^{(2)}(+M)$

$\Rightarrow$ $\chi^{(2)}$ is 3rd-rank c tensor

$$\chi^{(2)} = \begin{pmatrix} \cdot & \cdot & \cdot & \cdot & \cdot & \cdot \\ \cdot & \chi^{(2)}_{ijj} & \cdot & \cdot & \chi^{(2)}_{ijk} & \cdot \\ \cdot & \cdot & \cdot & \cdot & j \neq k & \cdot \end{pmatrix}$$

- Nondiagonal SHG tensor components are natural!
- $\Rightarrow$ **Large „nonlinear Kerr angles“** are expected.

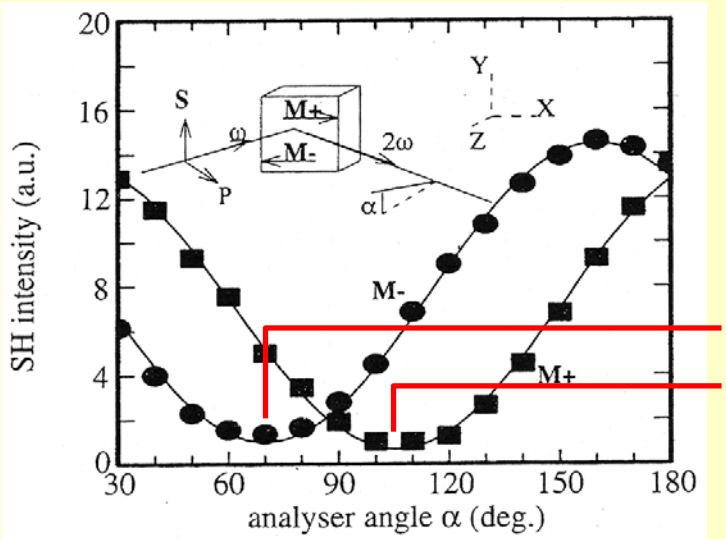

B. Koopmans et al. Phys. Rev. Lett. 74, 3692 (1995)

SHG on Magnetic Garnet Films

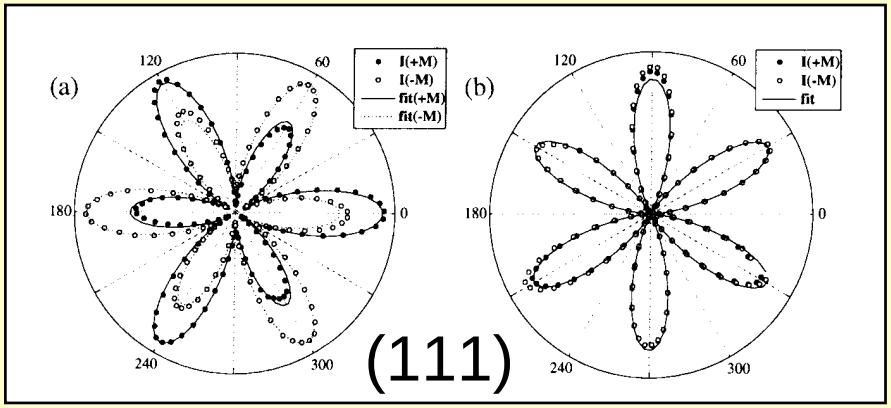

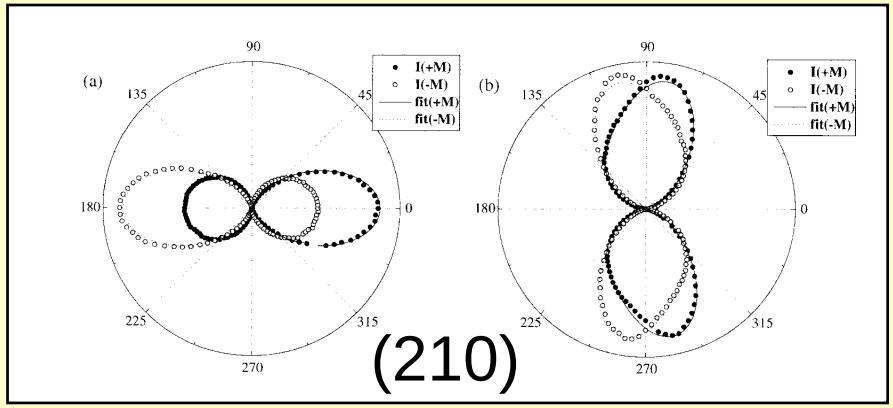

Incident light:

a) x polarized

b) y polarized

Table 3.6 Basic parameters of the samples

Substrate orientation	Film symmetry	Film composition	Lattice parameter (Å)		
			Film	Substrate	Misfit
(001)	4mm	$(YbPr)_3(FeGa)_5O_{12}$	12.4140	12.3787	0.0353
(111)	3m	$(YLuBi)_3(FeGa)_5O_{12}$	12.3720	12.3794	−0.0074
(210)	m	$(YPrLuBi)_3(FeGa)_5O_{12}$	12.5276	12.4789	0.0487
(110)	mm2	$(YBi)_3(FeGa)_5O_{12}$	12.382	12.377	0.005

A. Kirilyuk et al., Phys. Rev. B **63**, 184407 (2001)

MSHG is extremely sensitive to underlying symmetry!

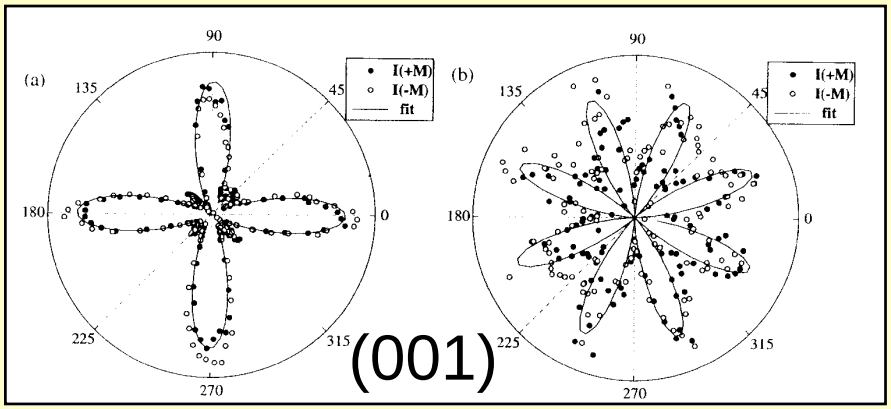

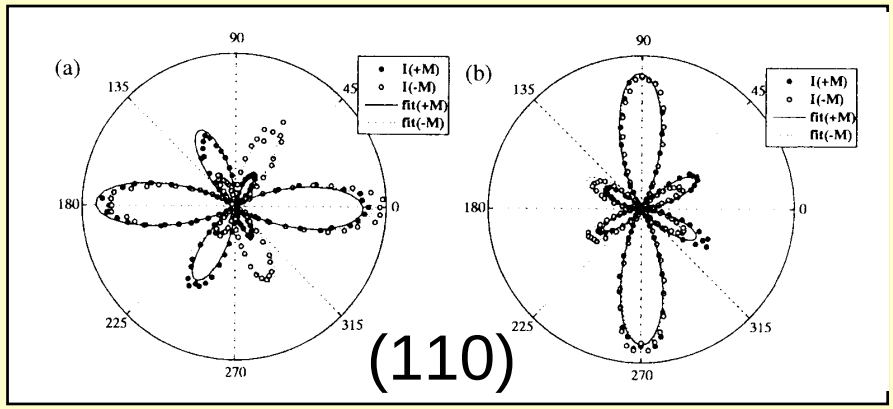

Magnetisation of Thin Films Derived from MSHG

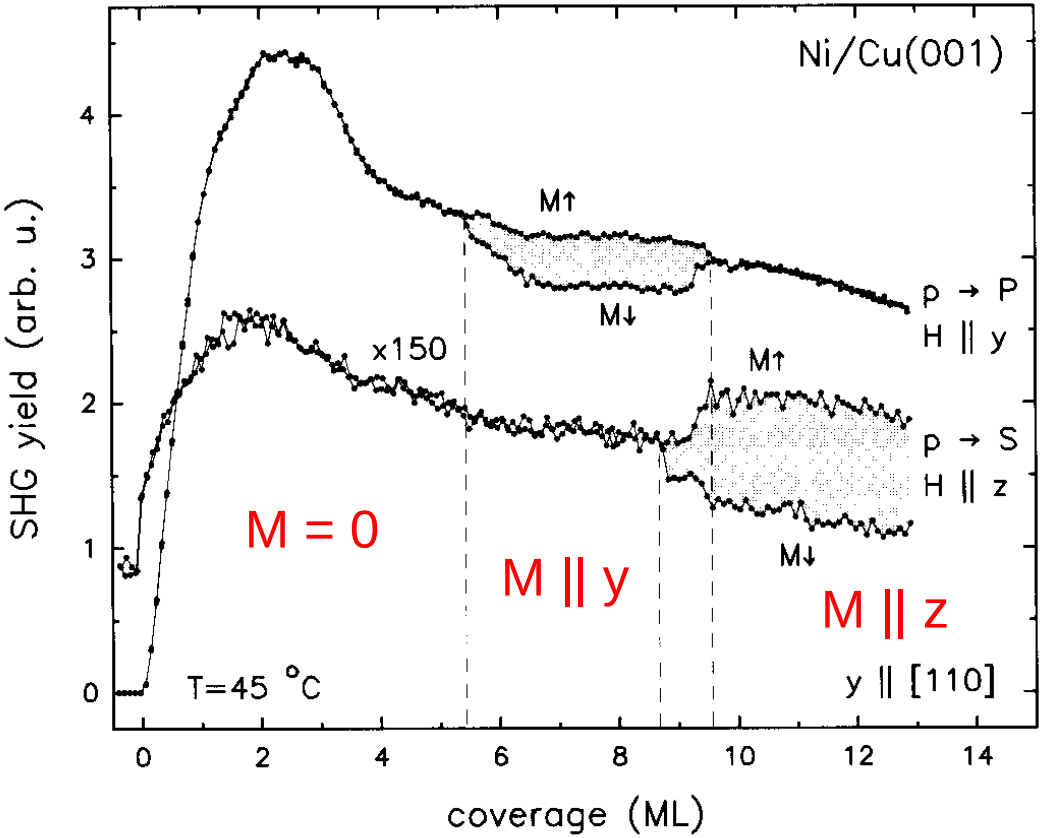

Fig. 4. SHG yield evolution during growth of Ni/Cu(001) for p_{in}-P_{out} and p_{in}-S_{out} polarization combinations. The external magnetic field was switched alternately between $+y$ and $-y$, or $+z$ and $-z$, respectively. The onset of in-plane magnetic order at 5.4 ML is reflected by the splitting of the two SH components for $H \| y$. The converging in-plane and diverging out-of-plane SH yield indicates the gradual reorientation of $\boldsymbol{M}$ from the y into the z direction between 8.7 to 9.6 ML

V. Jähnke et al. Appl. Phys. B 68, 485 (1999)

First Antiferromagnetic SHG Experiment

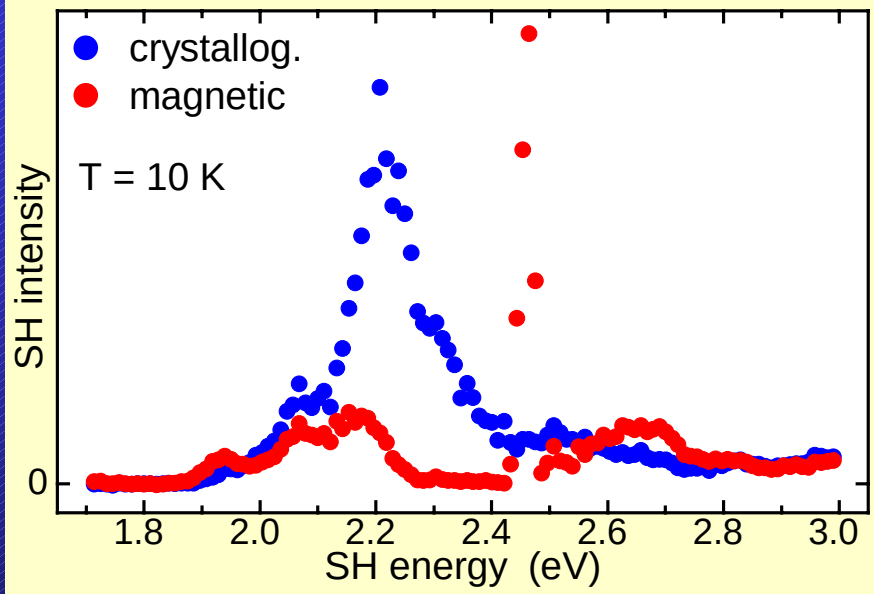

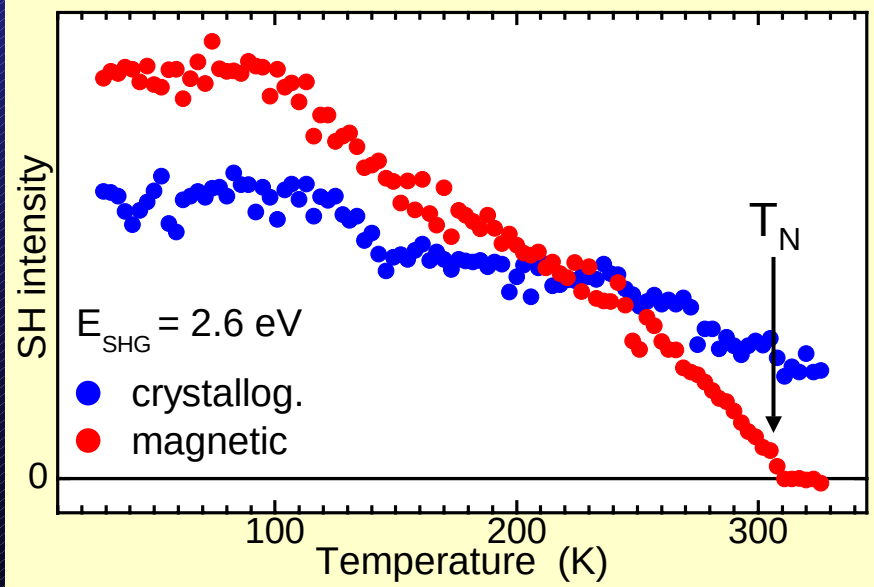

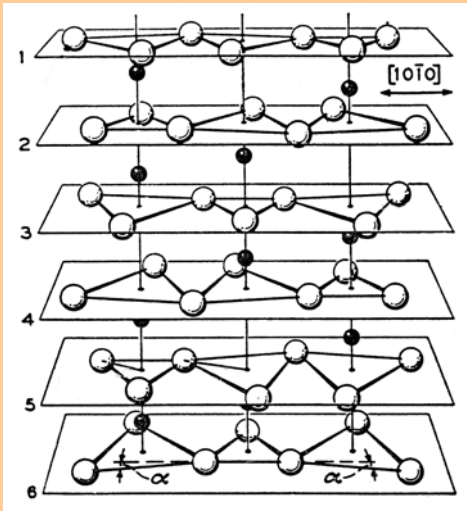

Cr_2O_3

Magnetoelectric antiferromagnet

T_N = 307.6 K

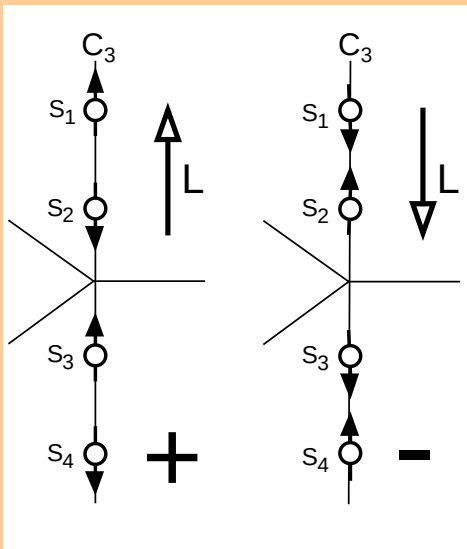

Magnetic structure

Two 180° domains (+/–)

Distinguished by spin re-versal

Magnetoelectric Correlations in Multiferroics

- Nonlinear Optics and Symmetry
- Cr_2O_3 as Case Study
- Experimental Setup
- Magnetoelectric Effects in Multiferroic $RMnO_3$
- Summary

Structure and Symmetry of Antiferromagnetic Cr_2O_3

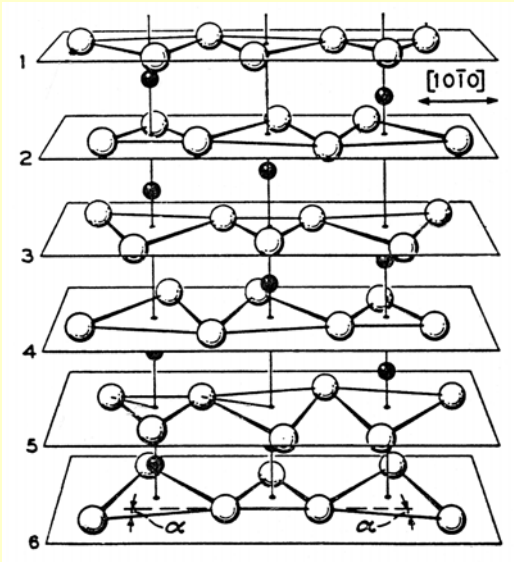

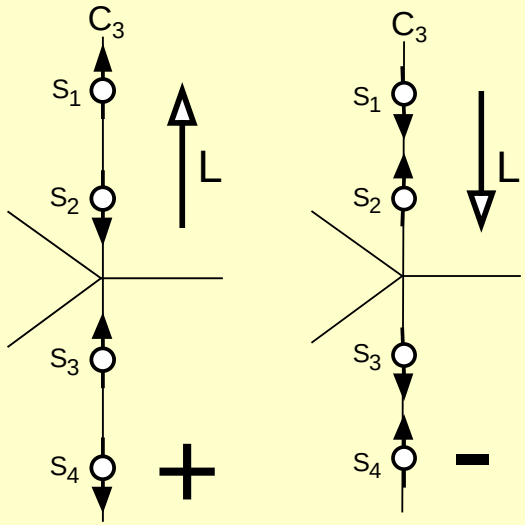

Cr_2O_3 is antiferromagnetic:
Néel temperature
$T_N = 307.6$ K

Two 180° domains (+/–),

symmetry $T > T_N$:
$D_{3d} = \bar{3}m$ with:
inversion I
time reversal T
and thus TI

Symmetry operations:

$\bar{3}m$: $1, \bar{1}, 3(2_\perp), \bar{3}(2_\perp), \pm 3_z, \pm\bar{3}_z$

$\underline{1}, \underline{\bar{1}}, \underline{3}(2_\perp), \underline{\bar{3}}(2_\perp), \pm\underline{3}_z, \pm\underline{\bar{3}}_z$

$\underline{\bar{3}m}$: $1, 3(2_\perp), \pm 3_z, \underline{\bar{1}}, \underline{\bar{3}}(2_\perp), \pm\underline{\bar{3}}_z$

symmetry $T < T_N$:
$D_{3d}(D_3) = \underline{\bar{3}m}$ with:
inversion I
time reversal T
but still TI

Wave Equation for Nonlinear Optics

Maxwell equations in matter with matter fields:

P (electric dipole moment, ED)

M (magnetic-dipole moment, MD)

Q (electric-quadrupole moment, EQ)

Leads to source term S in wave equation: (reaction of matter to light field at ω is generation of another light field at 2ω)

$$\mathrm{rot}\, H = j + \frac{\partial D}{\partial t} = j + \frac{\partial}{\partial t}\left(\varepsilon_0 E + P - \nabla Q\right)$$

$$\mathrm{rot}\, E = -\frac{\partial B}{\partial t} = \mu_0 \frac{\partial}{\partial t}\left(H + M\right)$$

$$P = P_L + P_{NL} = \varepsilon_0 \chi_L^e E + \varepsilon_0 \chi_{NL}^e EE$$

$$M = M_L + M_{NL} = 0 + \frac{\varepsilon_0 c}{n(\omega)} \chi_{NL}^m EE$$

$$\nabla Q = \nabla Q_L + \nabla Q_{NL} = 0 + -\frac{ic\varepsilon_0}{2\omega \cdot n(\omega)} \hat{e}_k \chi_{NL}^q EE$$

for SHG
$\hat{e}_k = \vec{k}/k$
$Q \equiv Q_{ij}$ (Tensor)
$M_L = 0$, no fun. Moment
$Q_L = 0$, negligible

$$\nabla \times \nabla \times E = \nabla(\nabla E) - \Delta E$$

$$= -\mu_0 \frac{\partial}{\partial t} \nabla \times (H + M)$$

$\nabla E = 0$, $j = \sigma E$, $\varepsilon = 1 + \chi_L^e$ ($\sigma \simeq 0$, Isolator)

$$\Delta E = \mu_0 \sigma \frac{\partial E}{\partial t} + \mu_0 \varepsilon_0 \varepsilon \frac{\partial^2 E}{\partial t^2} + \mu_0 \frac{\partial^2 P_{NL}}{\partial t^2} + \mu_0 \nabla \times \frac{\partial M_{NL}}{\partial t} - \mu_0 \frac{\partial^2 (\nabla Q_{NL})}{\partial t^2}$$

$$\Delta E - \frac{\varepsilon}{c^2} \frac{\partial^2 E}{\partial t^2} = \mu_0 \frac{\partial^2 P_{NL}}{\partial t^2} + \mu_0 \nabla \times \frac{\partial M_{NL}}{\partial t} - \mu_0 \frac{\partial^2 (\nabla Q_{NL})}{\partial t^2}$$

$$\left(\Delta - \frac{\varepsilon}{c^2} \frac{\partial^2}{\partial t^2}\right) E = S$$

Inhomogeneous wave eq. with source term S

Summary: SHG in Antiferromagnetic Cr_2O_3

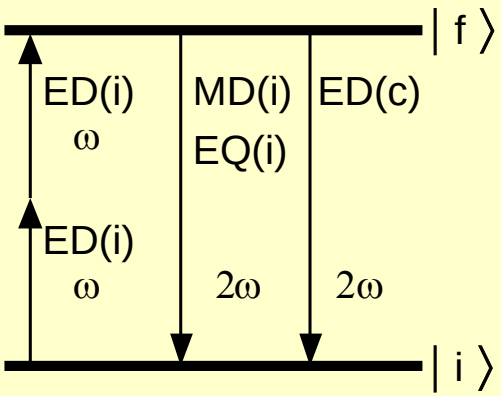

All temperatures:

$M_j(2\omega) \propto \chi_{ijk}^{m}(i)\, E_k(\omega)\, E_l(\omega)$ axial, time-invariant, rank 3

$Q_{ij}(2\omega) \propto \chi_{ijkl}^{q}(i)\, E_k(\omega)\, E_l(\omega)$ polar, time-invariant, rank 4

Only below $T_N = 307.6$ K:

$P_i(2\omega) \propto \chi_{ijk}^{e}(c)\, E_j(\omega)\, E_k(\omega)$ polar time-noninvar., rank 3

➤➤➤ Plane waves ($k \parallel c$)

$$\vec{M}_{NL} \propto \begin{pmatrix} \chi_m(i)E_-^2 \\ \chi_m(i)E_+^2 \\ 0 \end{pmatrix} \qquad \vec{\nabla}\hat{Q}_{NL} \propto \begin{pmatrix} \chi_q(i)E_-^2 \\ \chi_q(i)E_+^2 \\ 0 \end{pmatrix} \qquad \vec{P}_{NL} \propto \begin{pmatrix} \chi_e(c)E_-^2 \\ \chi_e(c)E_+^2 \\ 0 \end{pmatrix}.$$

➤➤➤ Wave equation $\vec{\nabla}\times(\vec{\nabla}\times\vec{E}) + \frac{\varepsilon}{c^2}\frac{\partial^2\vec{E}}{\partial t^2} = \vec{S}$ with source term S:

➤➤➤ $$\vec{S} = \mu_0 \frac{\partial^2 \vec{P}_{NL}}{\partial t^2} + \mu_0\left(\vec{\nabla}\times\frac{\partial \vec{M}_{NL}}{\partial t}\right) - \mu_0\left(\vec{\nabla}\cdot\frac{\partial^2 \hat{Q}_{NL}}{\partial t^2}\right) = 4\sqrt{2}\,\frac{\omega^2}{c^2}\begin{pmatrix} (-\chi_{m,q}(i) + i\chi_e(c))E_-^2 \\ (+\chi_{m,q}(i) + i\chi_e(c))E_+^2 \\ 0 \end{pmatrix}$$

➤➤➤ SHG intensity $I \propto |S|^2$:

$$I \propto (|\chi_{m,q}(i)|^2 + |\chi_e(c)|^2)\cdot(|E_+^4| + |E_-^4|)$$
$$- 2(\chi'_{m,q}(i)\chi''_e(c) - \chi''_{m,q}(i)\chi'_e(c))\cdot(|E_+^4| - |E_-^4|)$$

SHG in Antiferromagnetic Cr_2O_3

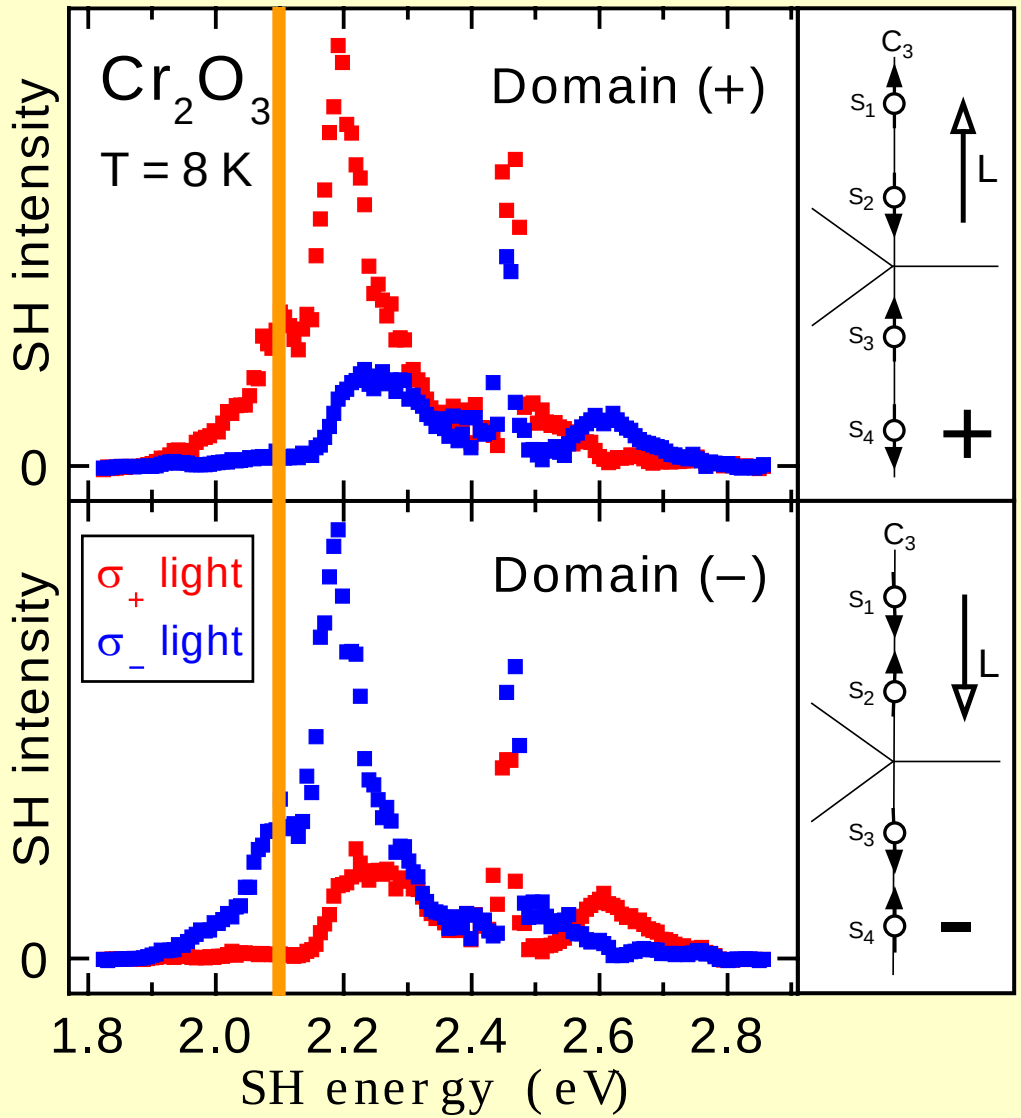

SH intensity for magnetic point group $\bar{3}m$ with $k \parallel z$:

$$I/I_0^2(L,\sigma) = C - \mathrm{sgn}(L)\,\mathrm{sgn}(\sigma)\cdot\Delta$$

Domain ± 1

Circular polarization ± 1

- Linear coupling to magnetic order parameter
- Distinction of antiferromagnetic 180° domains

Phys. Rev. Lett. **73**, 2127 (1994)

Antiferromagnetic 180° Domains in Cr_2O_3

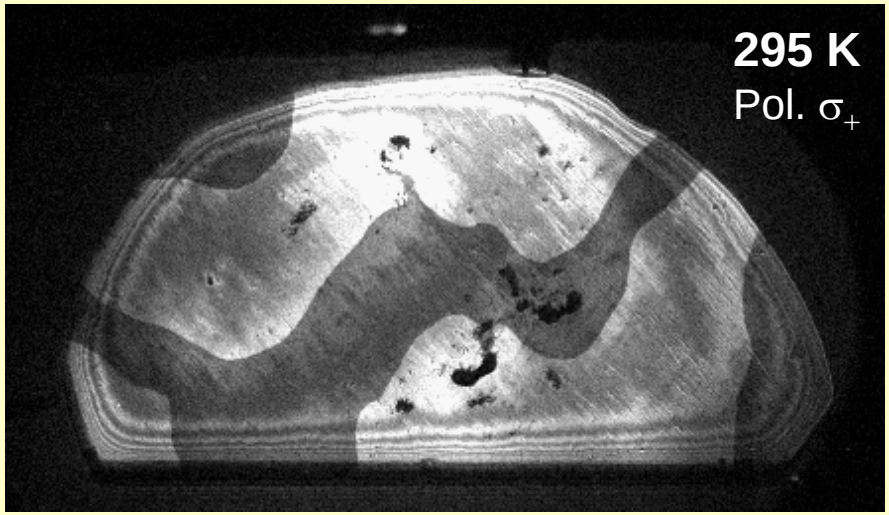

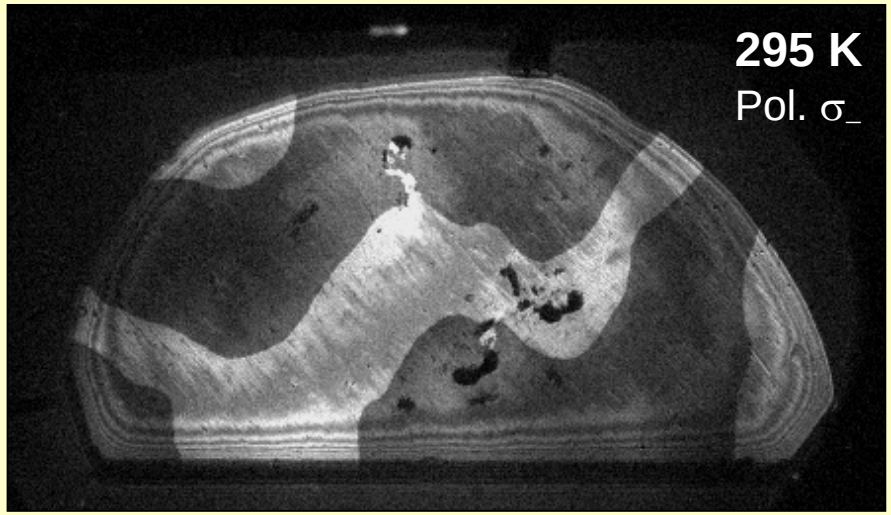

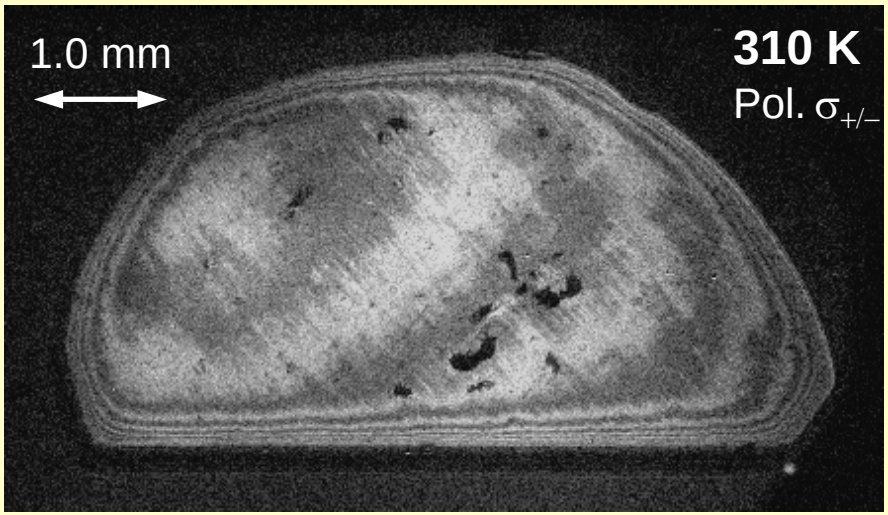

With SHG:

Exposure time:

~ 1 min

Resolution:

~ 1-10 μm

Appl. Phys. Lett. **66**, 2906 (1995)

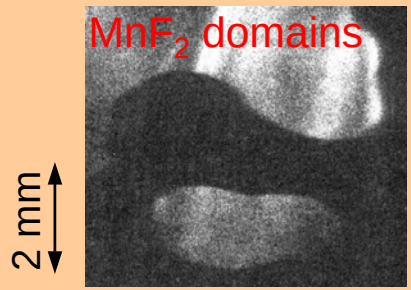

~24 h, 100 μm

Polarized neutrons

see: M. Schlenker, J. Baruchel, Ferroelectrics **162**, 299 (1994)

Seeing More with Nonlinear Optics

Antiferromagnetic Cr_2O_3 sample excited with infrared light ($\hbar\omega$ = 1.1 eV).

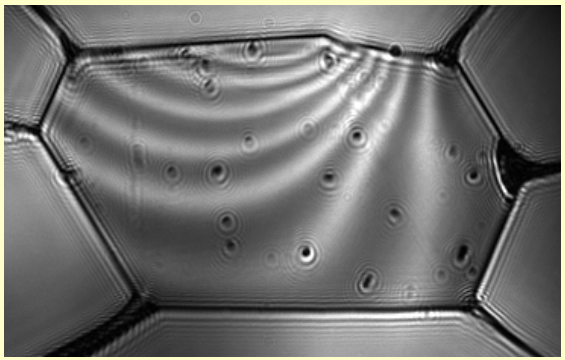

Incident light :	ω
Detected light :	ω

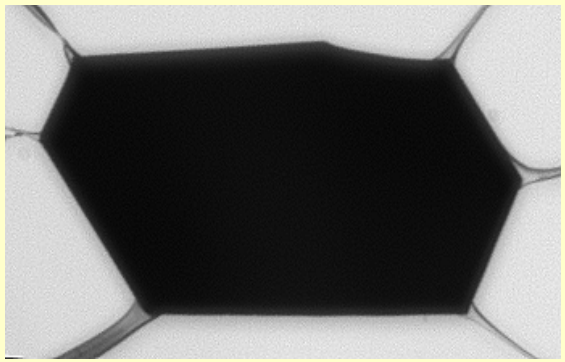

Incident light :	2ω
Detected light :	2ω

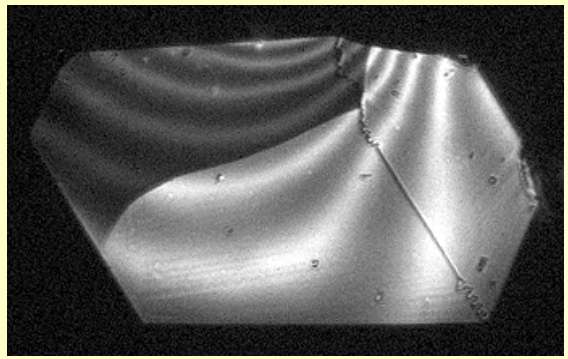

Incident light :	ω
Detected light :	2ω

Antiferromagnetic domains are visible with nonlinear experiment (second harmonic generation - SHG) only ➢ ➢ ➢ ➢ ➢ Novel physics!

Magnetoelectric Correlations in Multiferroics

- Nonlinear Optics and Symmetry
- Cr_2O_3 as Case Study
- **Experimental Setup**
- Magnetoelectric Effects in Multiferroic $RMnO_3$
- Summary

Experimental Setup for SHG

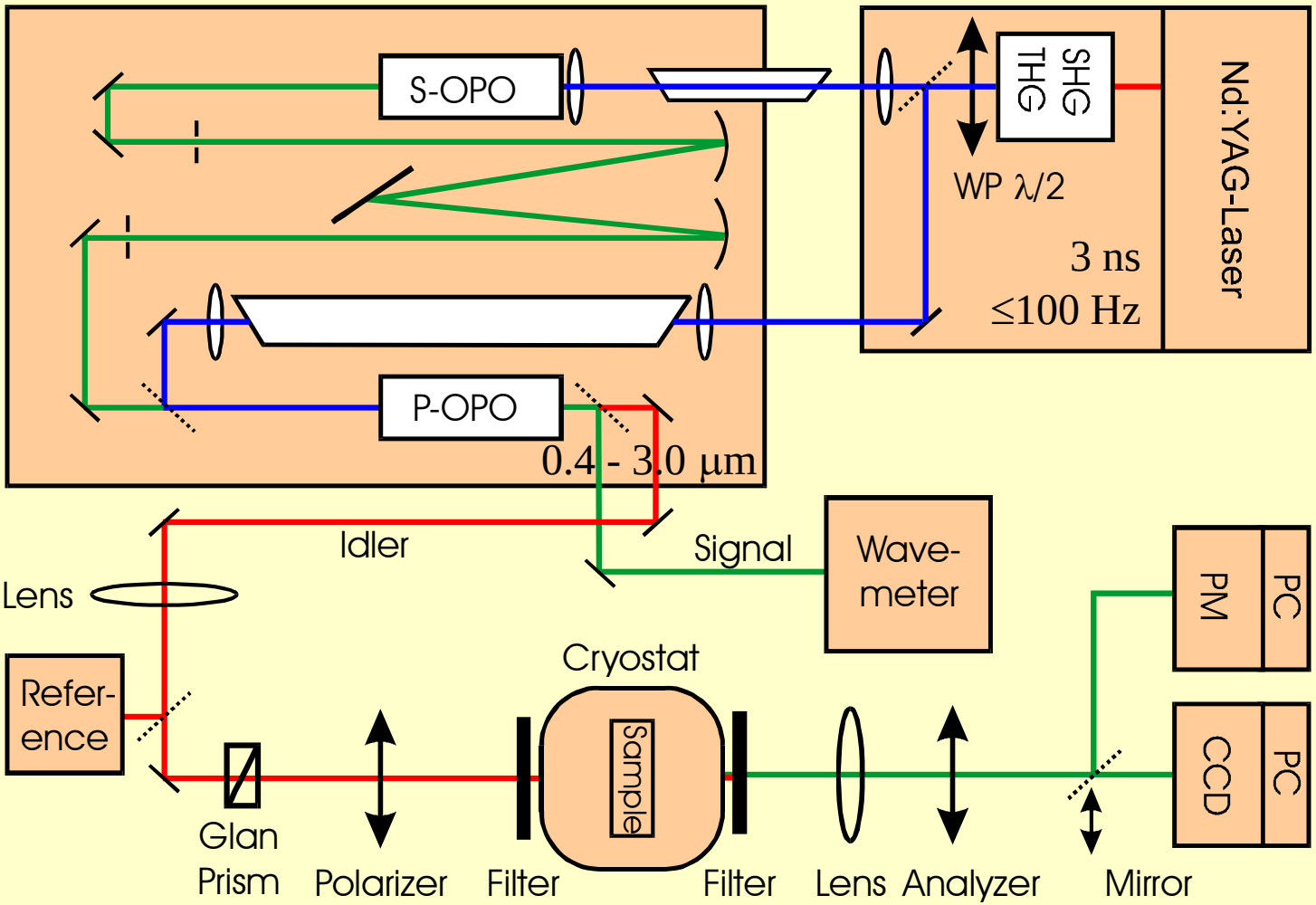

Optical Parametric Oscillator

Passive tunable narrow-band laser source in the range 400 nm – 3000 nm

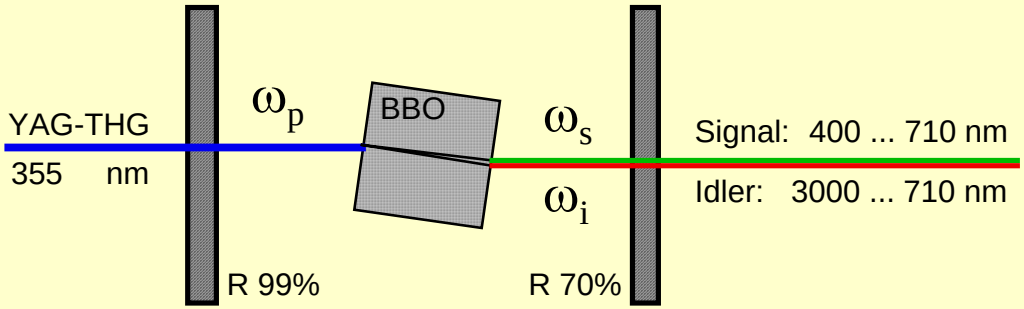

Parametric oscillation of transparent nonlinear crystal with high $\chi^{(2)}$-coefficients (here: beta-barium-borate β-BaB_2O_4)

Conservation of energy: $\hbar\omega_p = \hbar\omega_s + \hbar\omega_i \rightarrow \omega_p = \omega_s + \omega_i$

Conservation of momentum: $\hbar k_p = \hbar k_s + \hbar k_i \rightarrow n_p\omega_p = n_s\omega_s + n_i\omega_i$

n – refractive index $\rightarrow$ frequency tuning by rotation of crystal

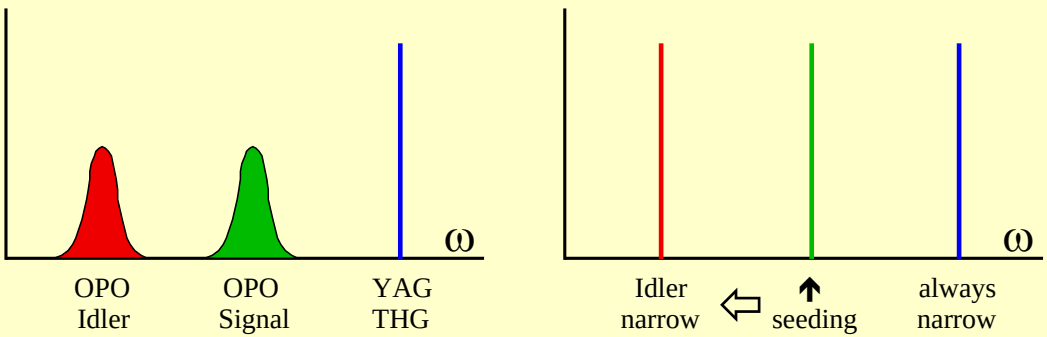

Reduction of linewidth (factor > 1000) by injection of second laser beam with signal frequency: "*seeding*"

Antiferromagnetic 180° Domains in $YMnO_3$

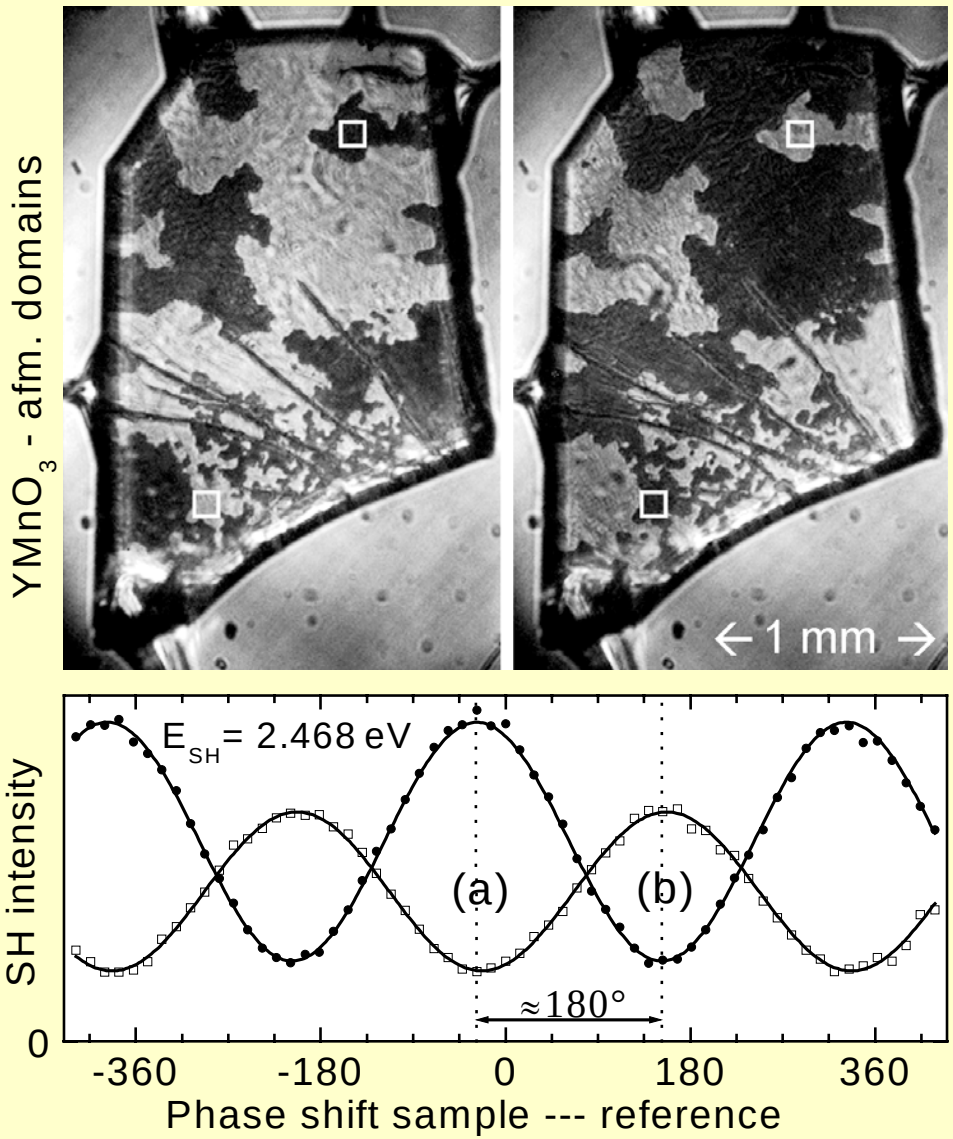

Second harmonic generation from opposite 180° domains:

$$+\chi^{(2)}(c) \leftrightarrow -\chi^{(2)}(c)$$

Leads to 180° phase shift in the magnetic SH light fields

SHG is the only convenient technique for imaging of antiferromagnetic 180° domains

Opt. Lett. **24**, 1520 (1999)

Setup for Phase-Sensitive SHG

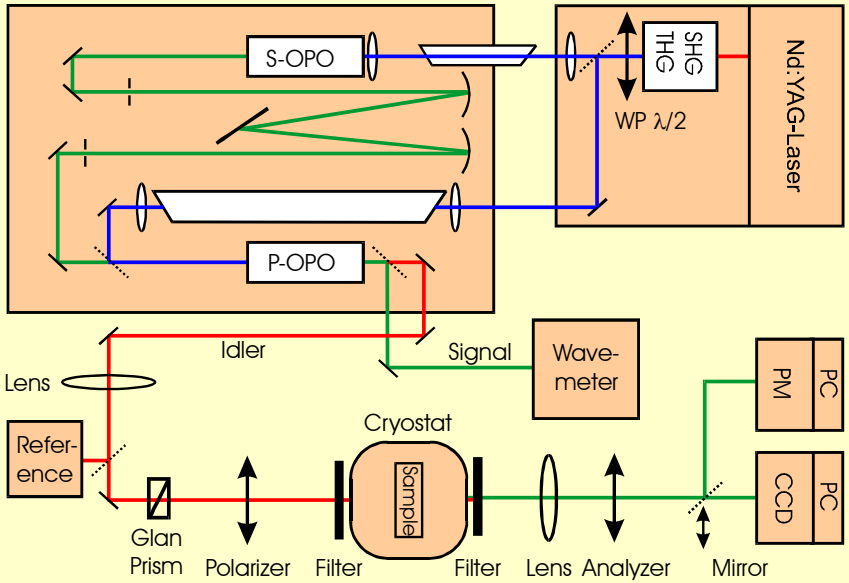

Basic setup with a pulsed Nd:YAG - OPO laser system (3 ns, ≤100 Hz, 0.4 - 3.0 μm)

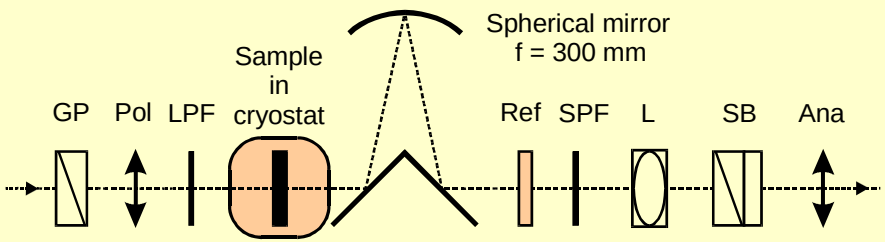

Achromatic beam imaging of sample on reference crystal in phase measurements

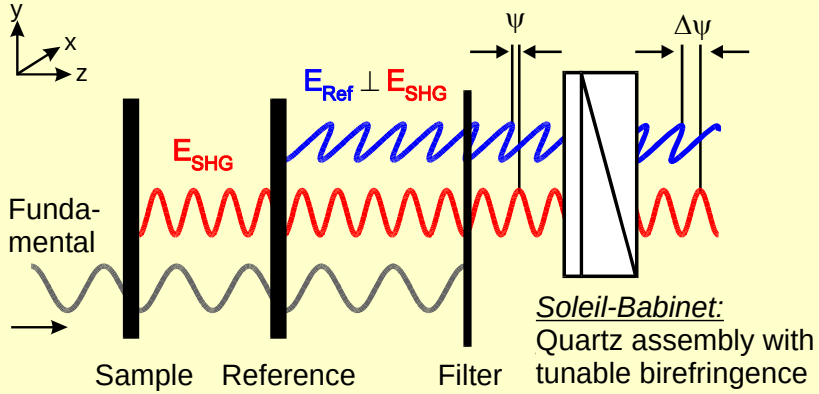

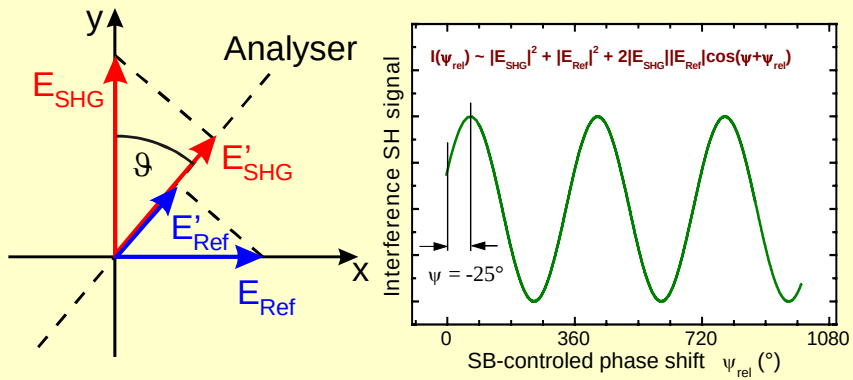

Holographic interference of SH signal from sample and SH reference wave from quartz crystal → amplitude and phase of signal wave

Opt. Lett. **24**, 1520 (1999), Opt. Lett. **29**, 41 (2004)

Phase- and Amplitude-Sensitive SHG

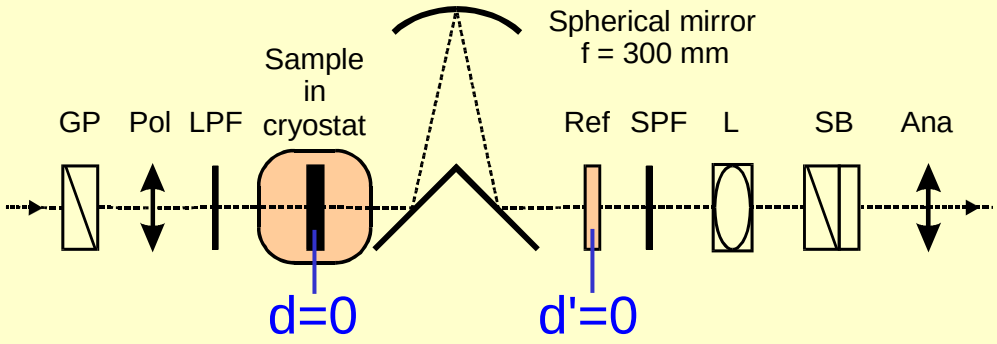

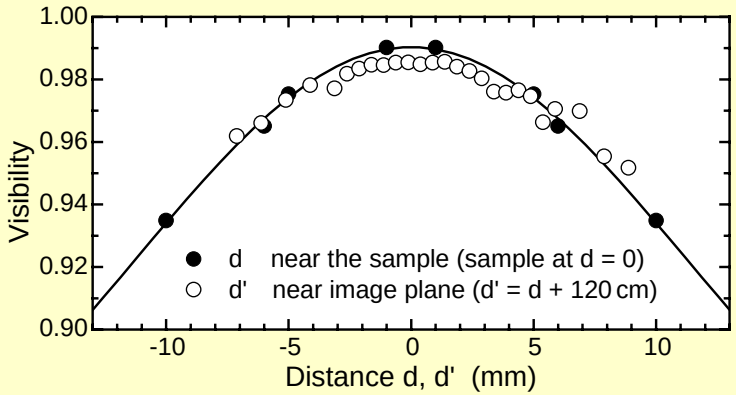

Magnetic SHG from sample

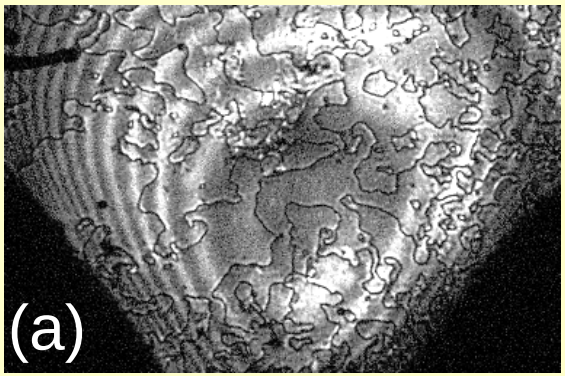

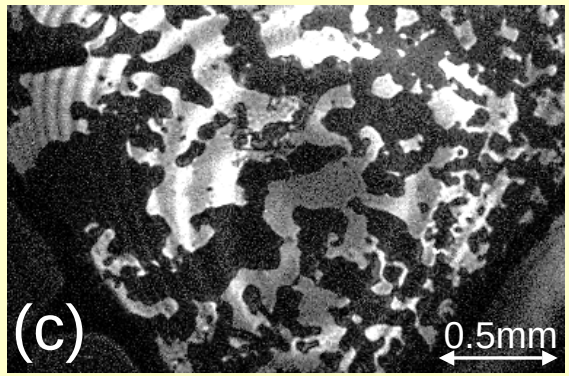

Signal + reference

Crystallographic SHG from reference quartz

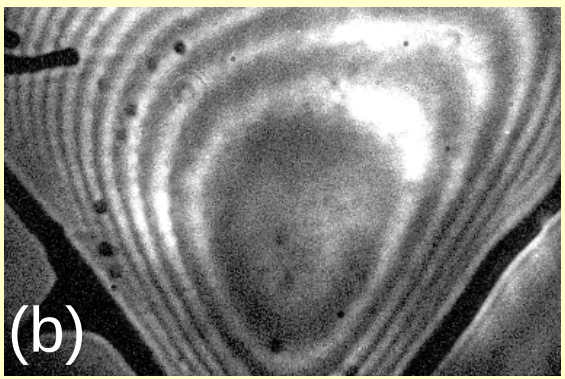

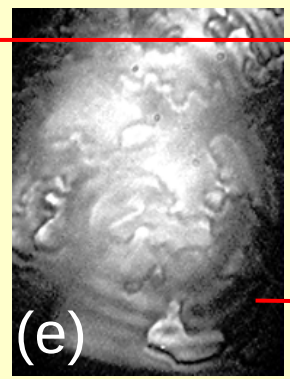

With imaging

Without imaging

Opt. Lett. **29**, 41 (2004)

Magnetoelectric Correlations in Multiferroics

- Nonlinear Optics and Symmetry
- Cr_2O_3 as Case Study
- Experimental Setup
- **Magnetoelectric Effects in Multiferroic $RMnO_3$**
- Summary

Magnetic Symmetry of Hexagonal $RMnO_3$

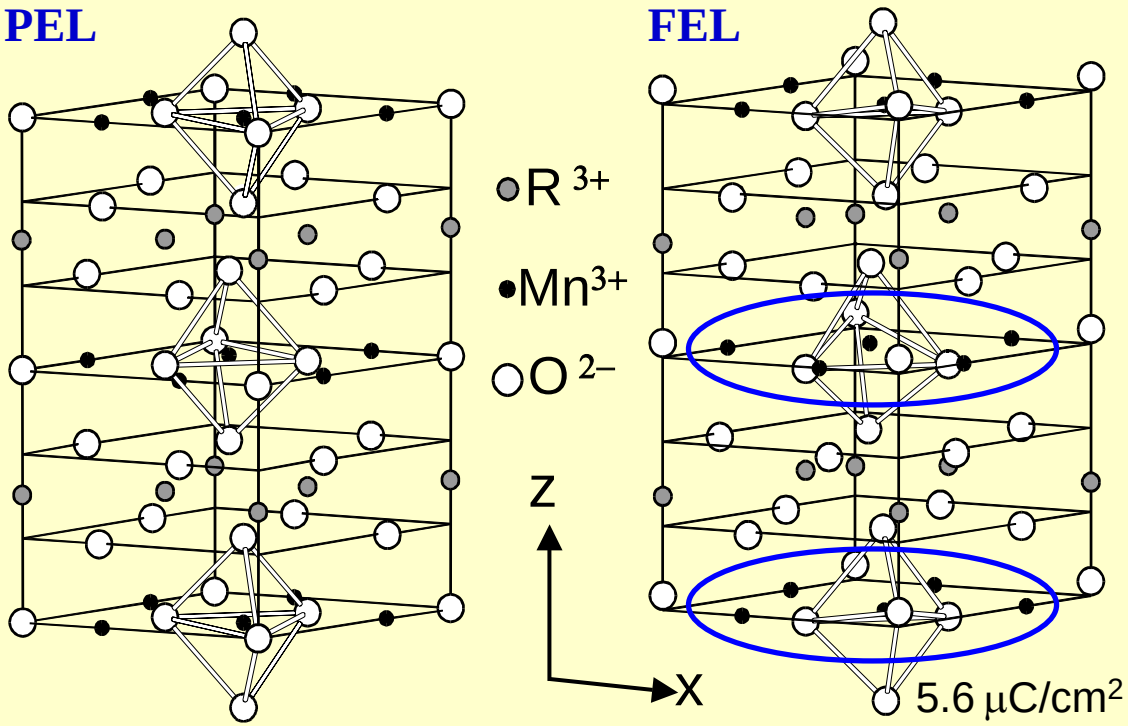

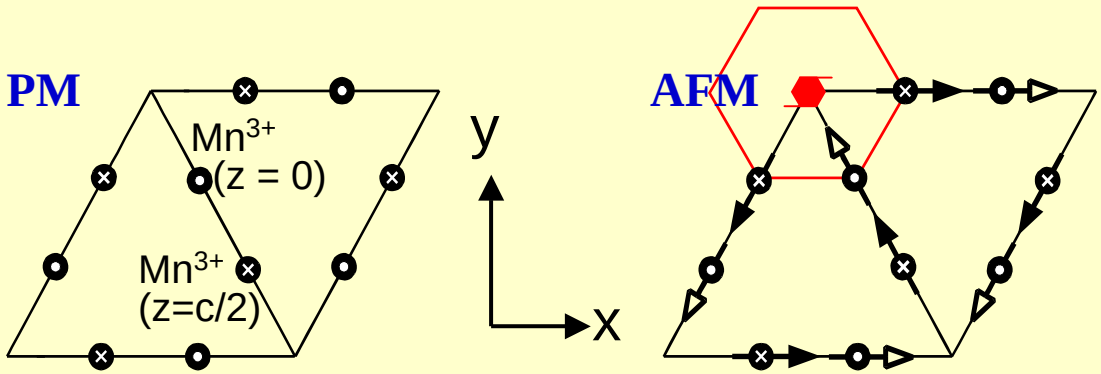

$RMnO_3$: A highly correlated and ordered system

- **Paraelectric → Ferroelectric** (PEL - FEL): T_C = 570 - 990 K
  Two 180° domains with $\pm P_z$
- **Para- → Antiferromagnetic** (PM - AFM): T_N = 70 - 130 K
  8 frustrated triangle structures

- Multiferroic/hexagonal for *R* = Sc,Y,In,Dy,Ho,Er,Tm,Yb,Lu
- Additional rare-earth order at ≈ 5 K for Dy, Ho, Er, Tm, Yb

Magnetic Structure and Selection Rules for SHG

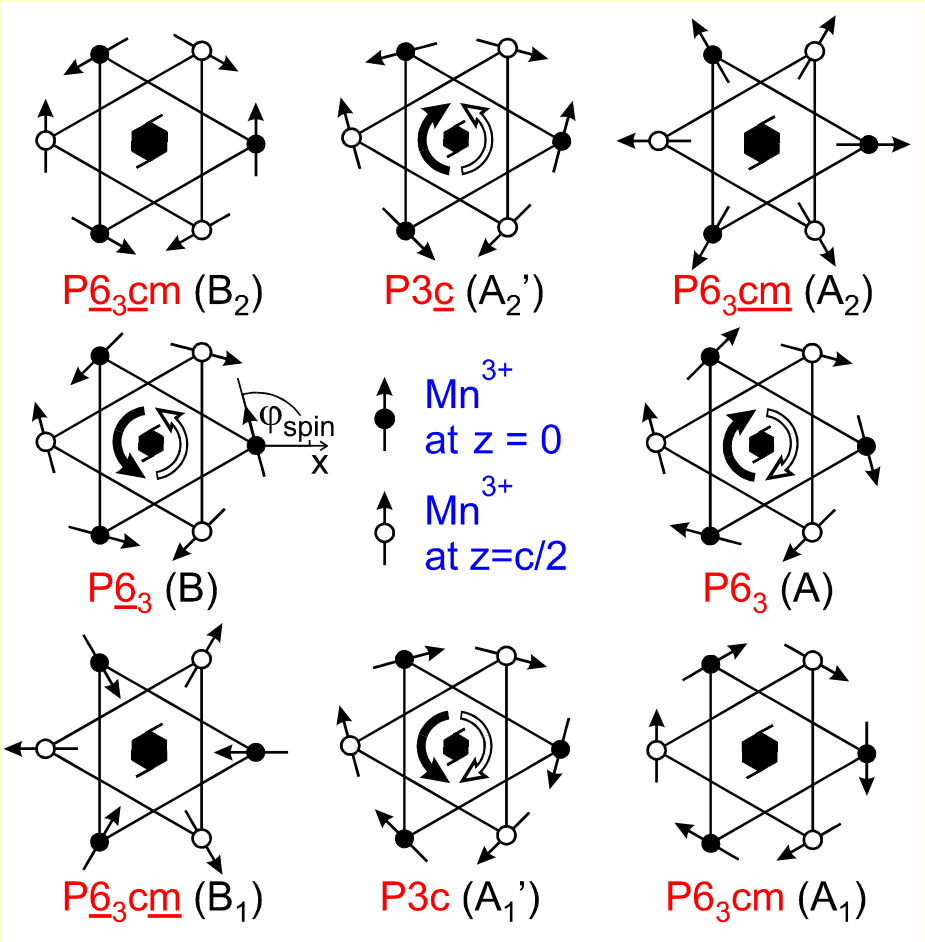

Different symmetry leads to different SHG contributions for all 8 structures

$$P_i(2\omega) \propto \chi_{ijk}\, E_j(\omega) E_k(\omega)$$

P6₃cm : $E_x(\omega) \rightarrow P_x(2\omega)$ $\sim \chi_{xxx}$

P6₃cm : $E_x(\omega) \rightarrow P_y(2\omega)$ $\sim \chi_{yyy}$

P6₃ : $E_x(\omega) \rightarrow P_x(2\omega) \oplus P_y(2\omega)$

P6₃.. : $E_x(\omega) \rightarrow 0$

usw.

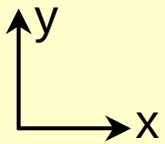

At least 8 different structures with different symmetries

Polarization of ingoing and outgoing light reveals the magnetic symmetry

SHG Spectrum and Magnetic Symmetry

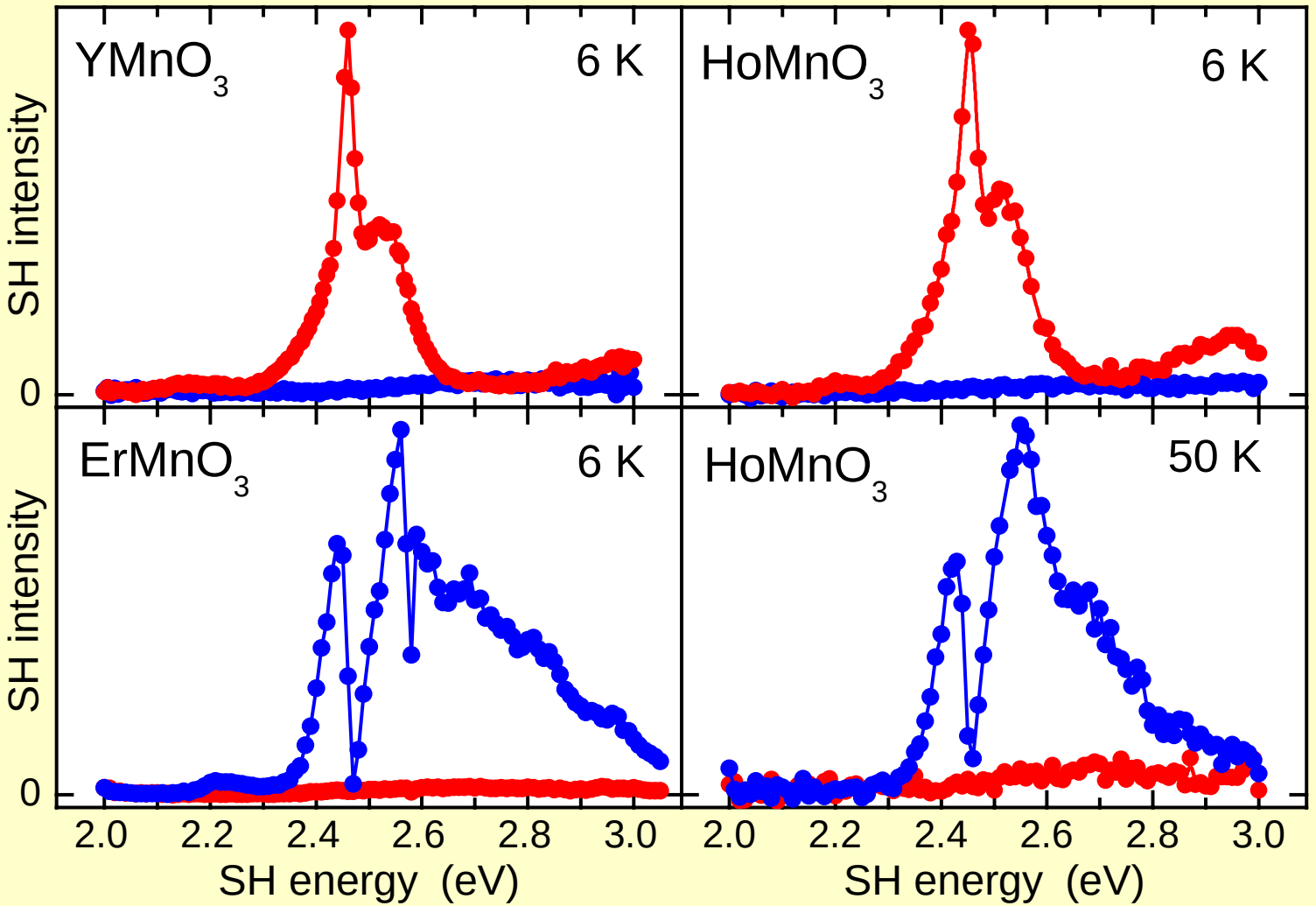

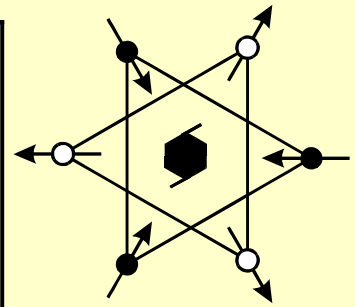

y polarized SHG

$P\underline{6_3}c\underline{m} \propto |\chi_{yyy}|^2$

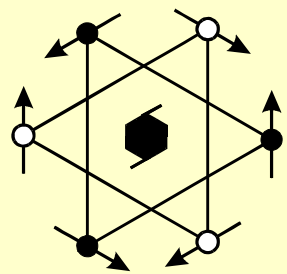

x polarized SHG

$P\underline{6_3}\underline{c}m \propto |\chi_{xxx}|^2$

Phys. Rev. Lett. **84**, 5620 (2000)

Magnetic Symmetry of Hexagonal $RMnO_3$

Second harmonic generation is the only technique capable of the determination of this magnetic phase diagram!

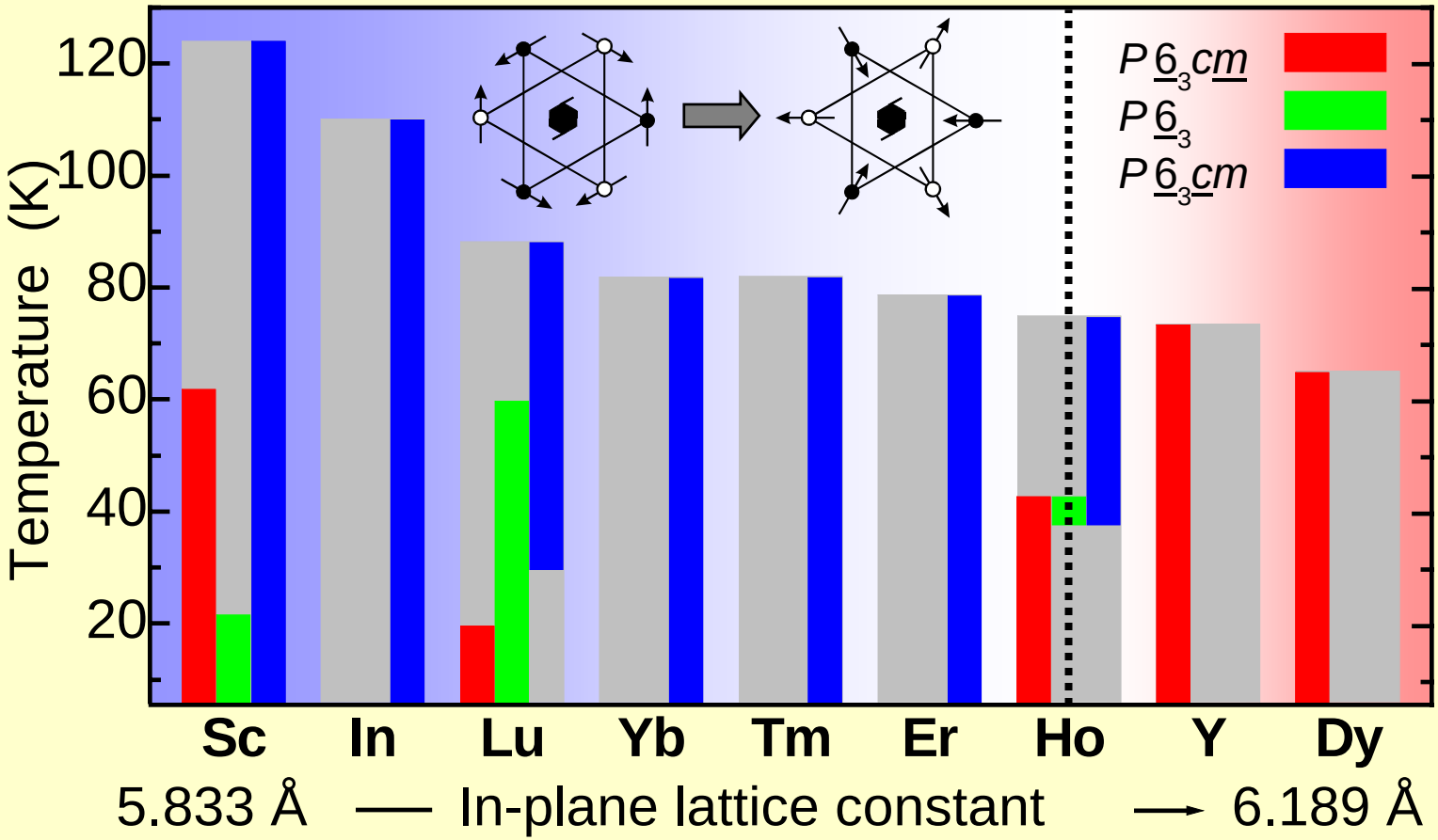

Phys. Rev. Lett. **84**, 5620 (2000)

Microscopic Origin of Two-Order-Parameter SHG

1. Trigonal bipyramidal field from O^{2-} ligands splits $3d^4$ state of free Mn^{3+} ion
2. Ferroelectric distortion of ligand field breaks local centrosymmetry and induces *p*-*d* mixing
3. Spin-orbit interaction mediates the coupling between the Mn^{3+} spins and the light waves at ω and 2ω
4. Leads to SHG coupling bilinearly to the antiferromagnetic and ferroelectric order parameters
5. Spectra dominated by excitonic Mn^{3+}– Mn^{3+} exchange
6. Constructive or destructive interference of excitonic subbands

INSTITUTE OF PHYSICS PUBLISHING JOURNAL OF PHYSICS: CONDENSED MATTER
J. Phys.: Condens. Matter 13 (2001) 3031–3055 www.iop.org/Journals/cm PII: S0953-8984(01)19896-6

Second-harmonic-generation spectra of the hexagonal manganites $RMnO_3$

Takako Iizuka-Sakano[1], Eiichi Hanamura[2] and Yukito Tanabe[3]

[1] Electrotechnical Laboratory, 1-1-4 Umezono, Tsukuba, Ibaraki 305-8568, Japan
[2] Chitose Institute of Science and Technology and CREST, JST (Japan Science and Technology Corporation), 785-65 Bibi, Chitose-City, Hokkaido 066-8655, Japan
[3] Department of Applied Physics, University of Tokyo, 7-3-1 Hongo, Bunkyo-ku, Tokyo 113-8656, Japan

Received 8 December 2000

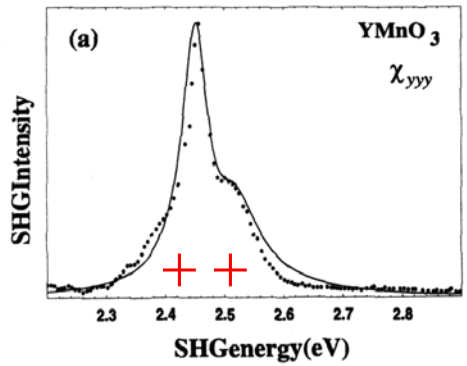

$$\epsilon_0\chi^{(1)}_{yyy} = -i\frac{3}{2}c^3c'pq(S_x)$$
$$\times\left[\sum_{\nu}\frac{(\nu_1\lambda/\Delta E(1,4)-\nu_2\lambda/\Delta E(2,3))}{(E(\nu E_2)-2\hbar\omega)\,\Delta E}\right.$$
$$\times(\nu_1 v_{zx}/\Delta E(1,3)-\nu_2 v_{zx}/\Delta E(2,4))$$
$$+\sum_{\mu}\frac{(\mu_1 v_{zx}/\Delta E(1,3)-\mu_2 v_{zx}/\Delta E(2,4))}{(E(\mu E_1)-2\hbar\omega)\,\Delta E}$$
$$\left.\times(\mu_1\lambda/\Delta E(1,4)-\mu_2\lambda/\Delta E(2,3))\right].$$

Spins along x

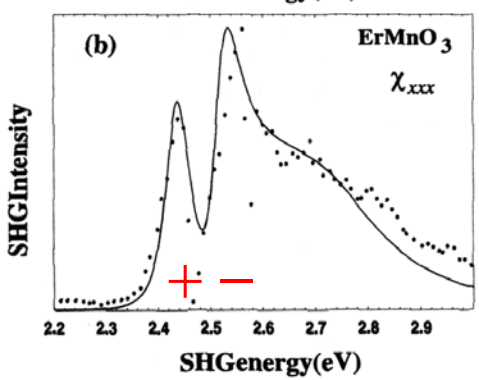

$$\epsilon_0\chi^{(1)}_{xxx} = i\frac{3}{2}c^3c'pq(S_y)$$
$$\times\left[\sum_{\nu}\frac{(\nu_1\lambda/\Delta E(1,3)-\nu_2\lambda/\Delta E(2,4))}{(E(\nu E_2)-2\hbar\omega)\,\Delta E}\right.$$
$$\times(\nu_1 v_{zx}/\Delta E(1,3)-\nu_2 v_{zx}/\Delta E(2,4))$$
$$-\sum_{\mu}\frac{(\mu_1 v_{zx}/\Delta E(1,3)-\mu_2 v_{zx}/\Delta E(2,4))}{(E(\mu E_1)-2\hbar\omega)\,\Delta E}$$
$$\left.\times(\mu_1\lambda/\Delta E(1,3)-\mu_2\lambda/\Delta E(2,4))\right].$$

Spins along y

Magnetic Phase Diagram of $ErMnO_3$

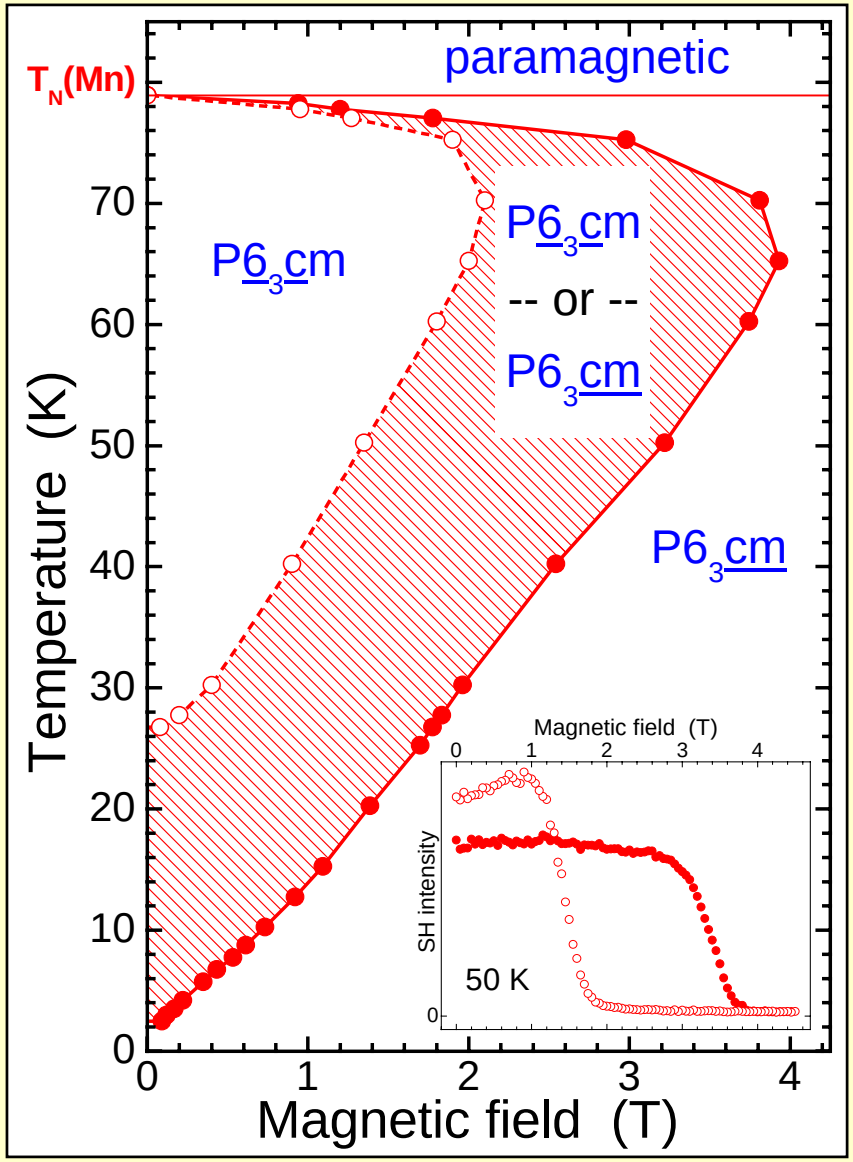

Magnetic reorientation of Mn^{3+} sublattice in magnetic field along the hexagonal axis

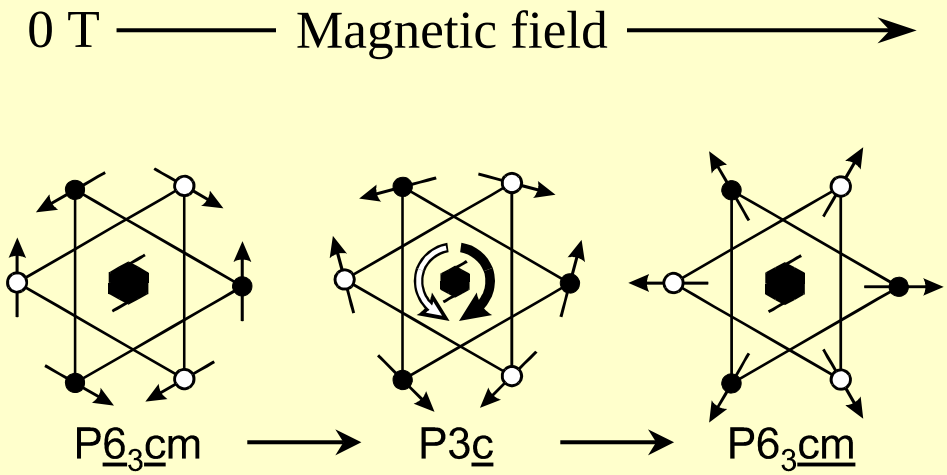

Magnetoelectric effect:

forbidden → **allowed**

Phys. Rev. Lett. **88**, 027203 (2002)

H/T Phase Diagram of Hexagonal $RMnO_3$

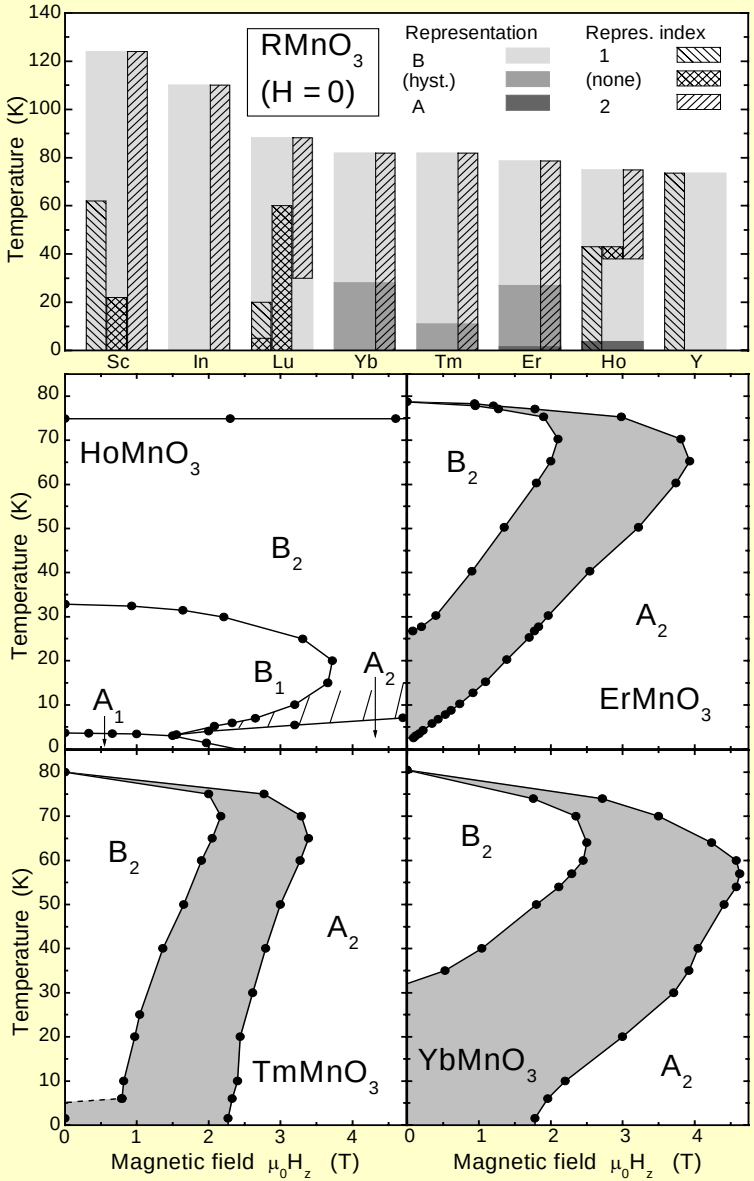

J. Appl. Phys. **83**, 8194 (2003)

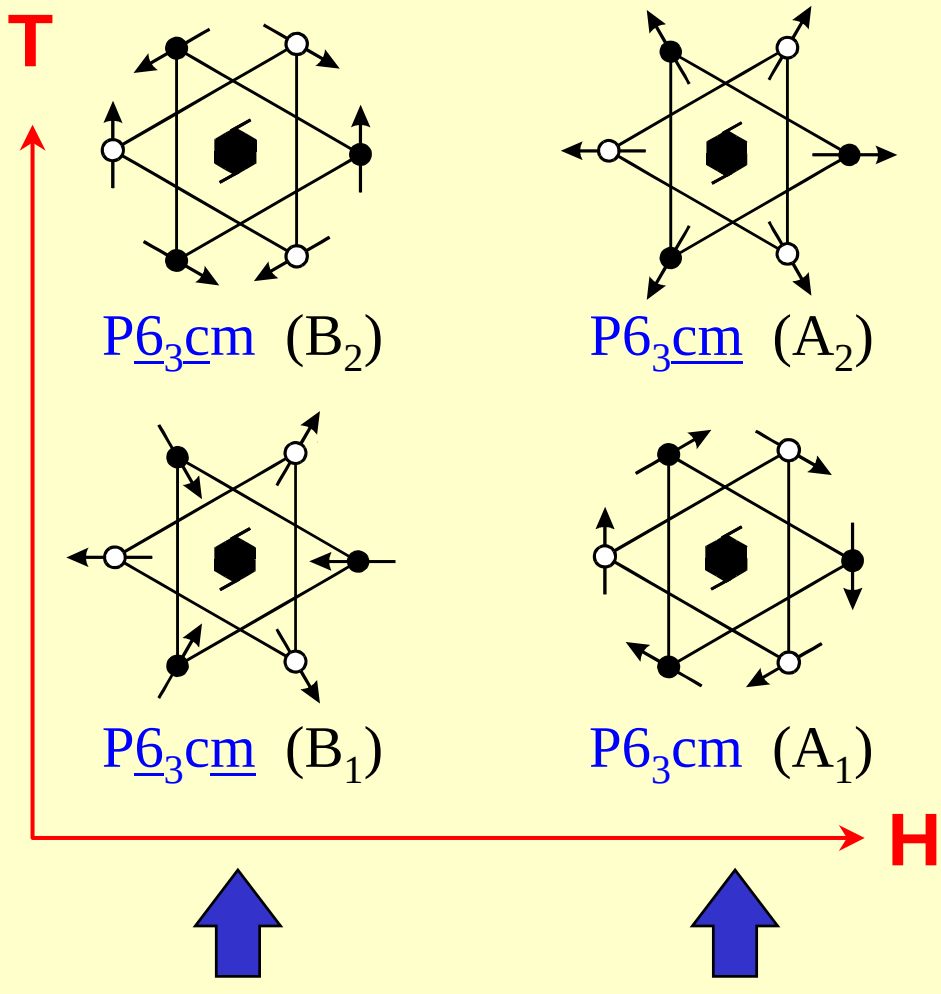

3*d* - 4*f* Superexchange in Dielectric $ErMnO_3$

Ferroelectric distortion neglected:

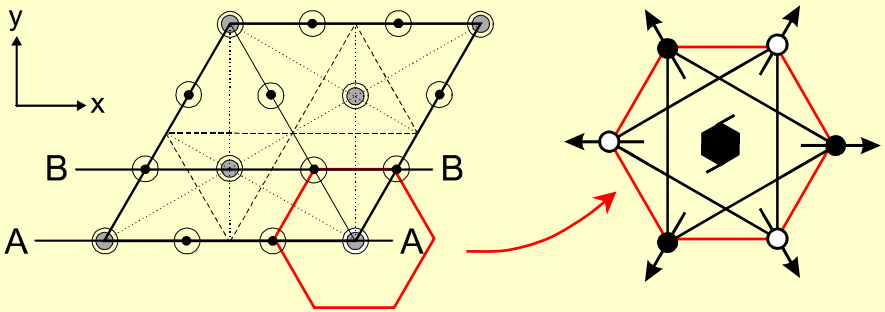

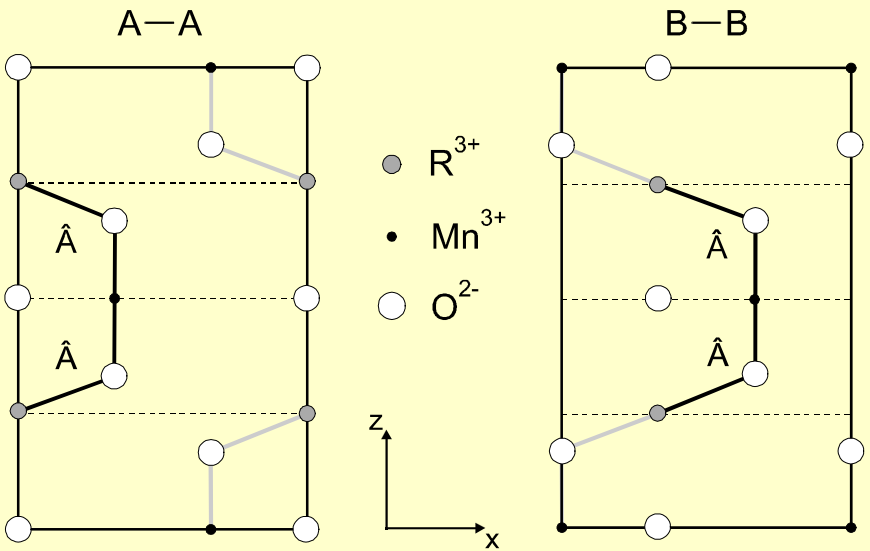

Phys. Rev. Lett. **88**, 027203 (2002)

$$H_{\rm ex} = \sum_{k=3m,3} \sum_{i_k=1}^{\substack{4\,(k=3)\\2\,(k=3m)}} \sum_{j=1}^{6} \vec{S}^{R^k(i_k)}\, \hat{A}^{k,i_k,j}\, \vec{S}^{\rm Mn(j)}$$

- k: R sites with 3 and 3m symmetries
- i_k: all R ions at k sites (4+2)
- j: 6 Mn ions neighboring an R ion
- A: Mn-R exchange matrix (4 types)
- S: spins of Mn and R ions

Only one 3*d*–4*f* superexchange path: Â

Superexchange energy:

$$H_{\rm ex} = 6\ell\, S^{\rm Er} S^{\rm Mn} \left[(A_{zx} - A_{zx}) - (A_{zx} - A_{zx})\right]$$

➤➤➤ $H_{\rm ex} = 0$ ◅◅◅

- Cancellation of the contributions to the superexchange energy
- Because of the equality of all the superexchange paths

3*d* - 4*f* Superexchange in Ferroelectric $ErMnO_3$

Ferroelectric distortion included:

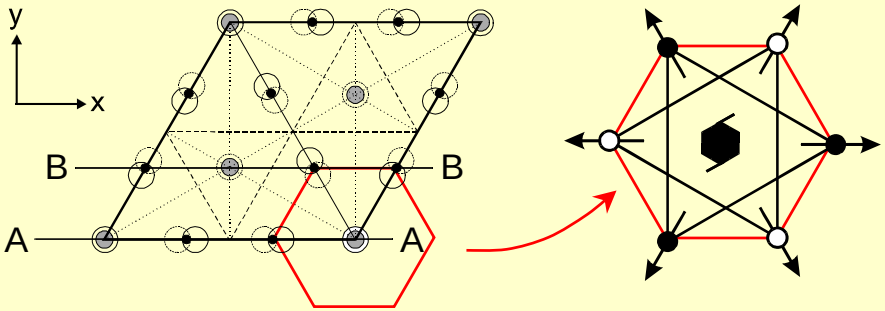

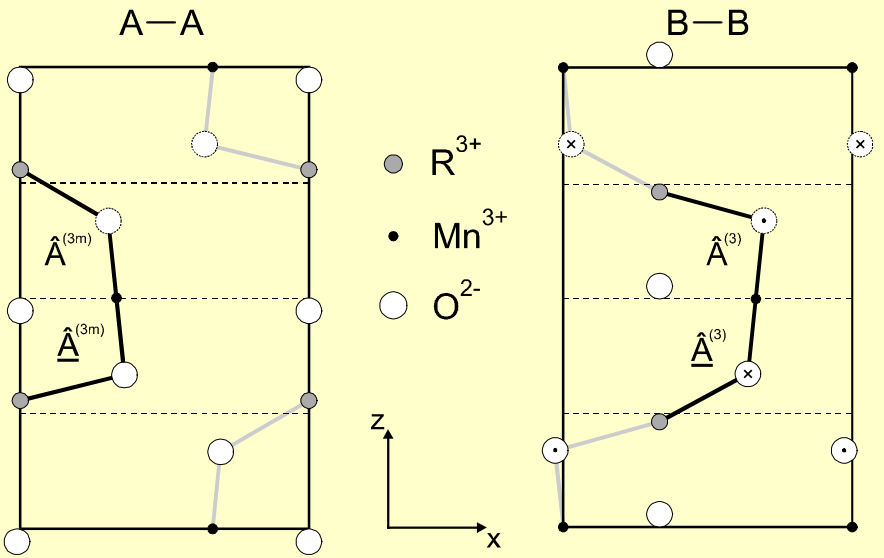

Phys. Rev. Lett. **88**, 027203 (2002)

$$H_{\text{ex}} = \sum_{k=3m,3} \sum_{i_k=1}^{\substack{4\,(k=3)\\2\,(k=3m)}} \sum_{j=1}^{6} \vec{S}^{R^k(i_k)}\, \hat{A}^{k,i_k,j}\, \vec{S}^{\text{Mn}(j)}$$

k: R sites with 3 and 3m symmetries
i_k: all R ions at k sites (4+2)
j: 6 Mn ions neighboring an R ion
A: Mn-R exchange matrix (4 types)
S: spins of Mn and R ions

Four exchange paths: $\hat{A}^{3m}$, $\underline{\hat{A}}^{3m}$, $\hat{A}^{3}$, $\underline{\hat{A}}^{3}$

Superexchange energy:

$$H_{\text{ex}} = 6\ell\, S^{\text{Er}} S^{\text{Mn}} \left[\left(A_{zx}^{3m} - \underline{A}_{zx}^{3m}\right) - \left(A_{zx}^{3} - \underline{A}_{zx}^{3}\right) \right]$$

➤➤➤ $H_{\text{ex}} \neq 0$ ◅◅◅

- Ferroelectric distortion breaks symmetry of Er^{3+}–Mn^{3+} superexchange
- Represents magnetoelectric interaction on the microscopic scale

Phase Transitions by 'Giant' Magnetoelectric Effect

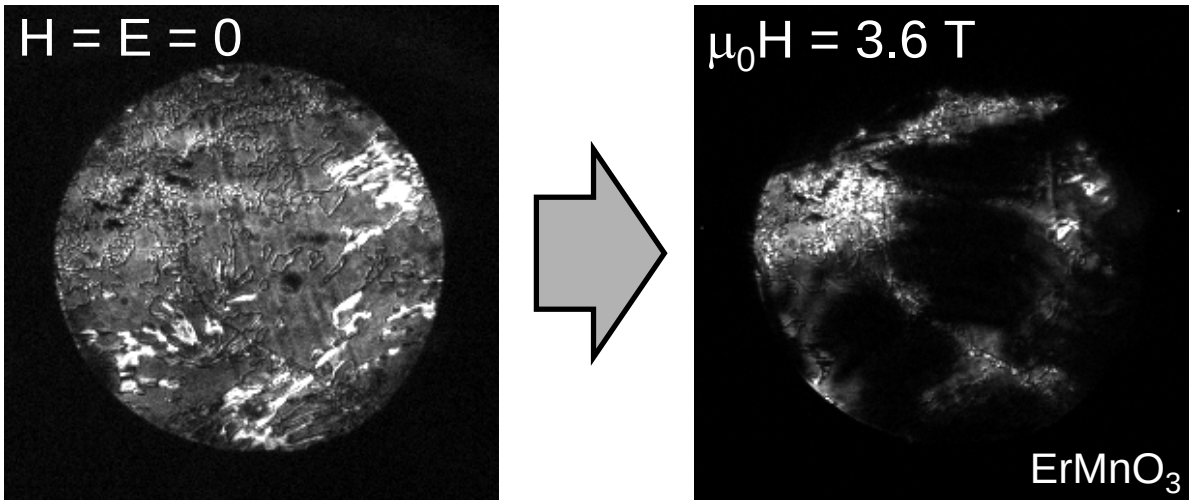

Magnetic phase control excerted by applied magnetic field

$$H_{ME} = \alpha_{zz} P_z M_z$$

- Mn^{3+} spin reori-entation makes magnetoelectric effect allowed
- Magnetoelectric contribution lowers ground state energy
- Magnetoelectric effect triggers phase transition

Phase Transitions by 'Giant' Magnetoelectric Effect

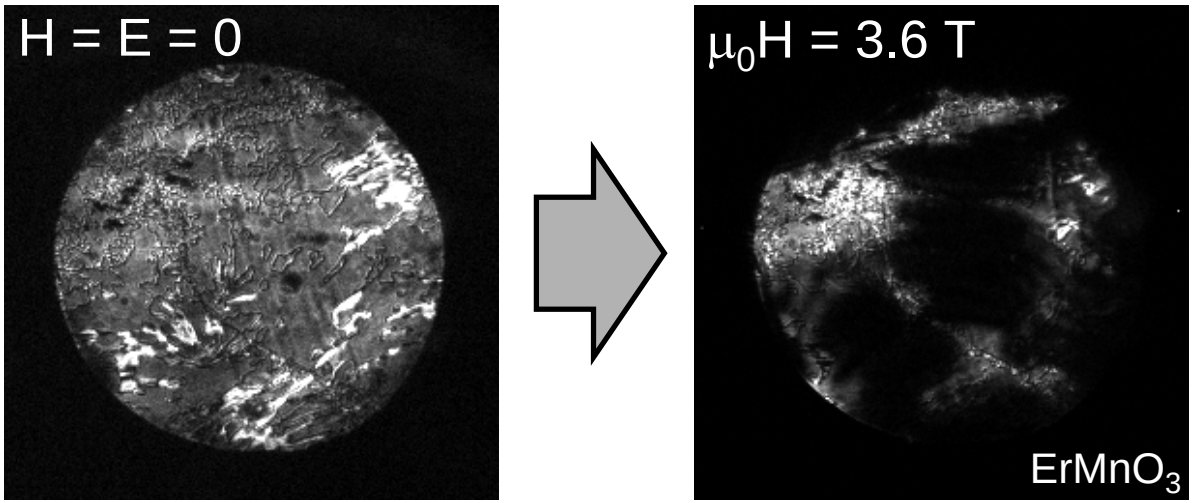

Magnetic phase control excerted by applied magnetic field

Also possible by applied electric field???

$$H_{ME} = \alpha_{zz} P_z M_z$$

- Mn^{3+} spin reori-entation makes magnetoelectric effect allowed
- Magnetoelectric contribution lowers ground state energy
- Magnetoelectric effect triggers phase transition

Phase Transitions by 'Giant' Magnetoelectric Effect

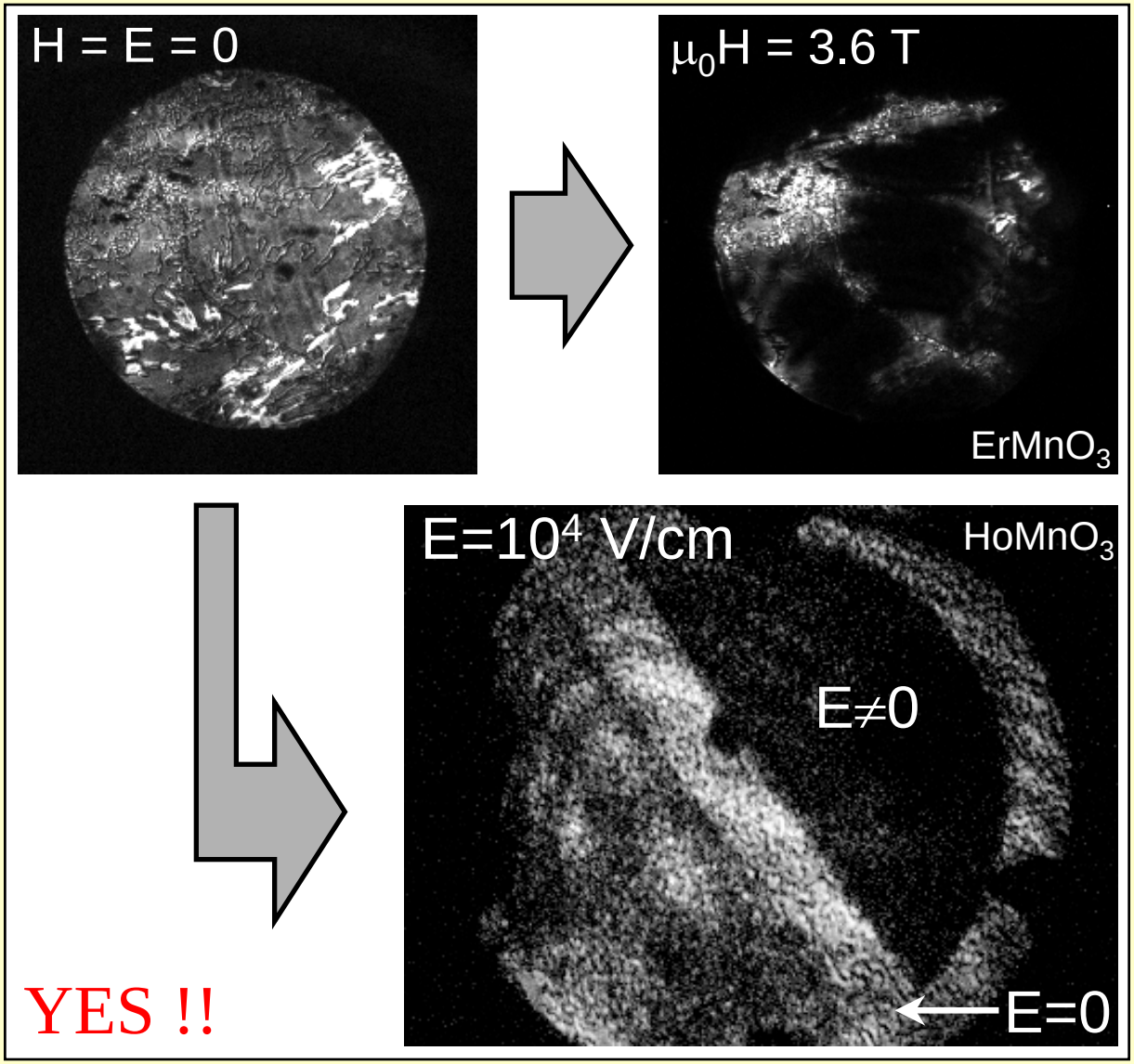

$$H_{ME} = \alpha_{zz} P_z M_z$$

- Mn^{3+} spin reori-entation makes magnetoelectric effect allowed
- Magnetoelectric contribution lowers ground state energy
- Magnetoelectric effect triggers phase transition

Magnetic Phase Control by Electric Field in $HoMnO_3$

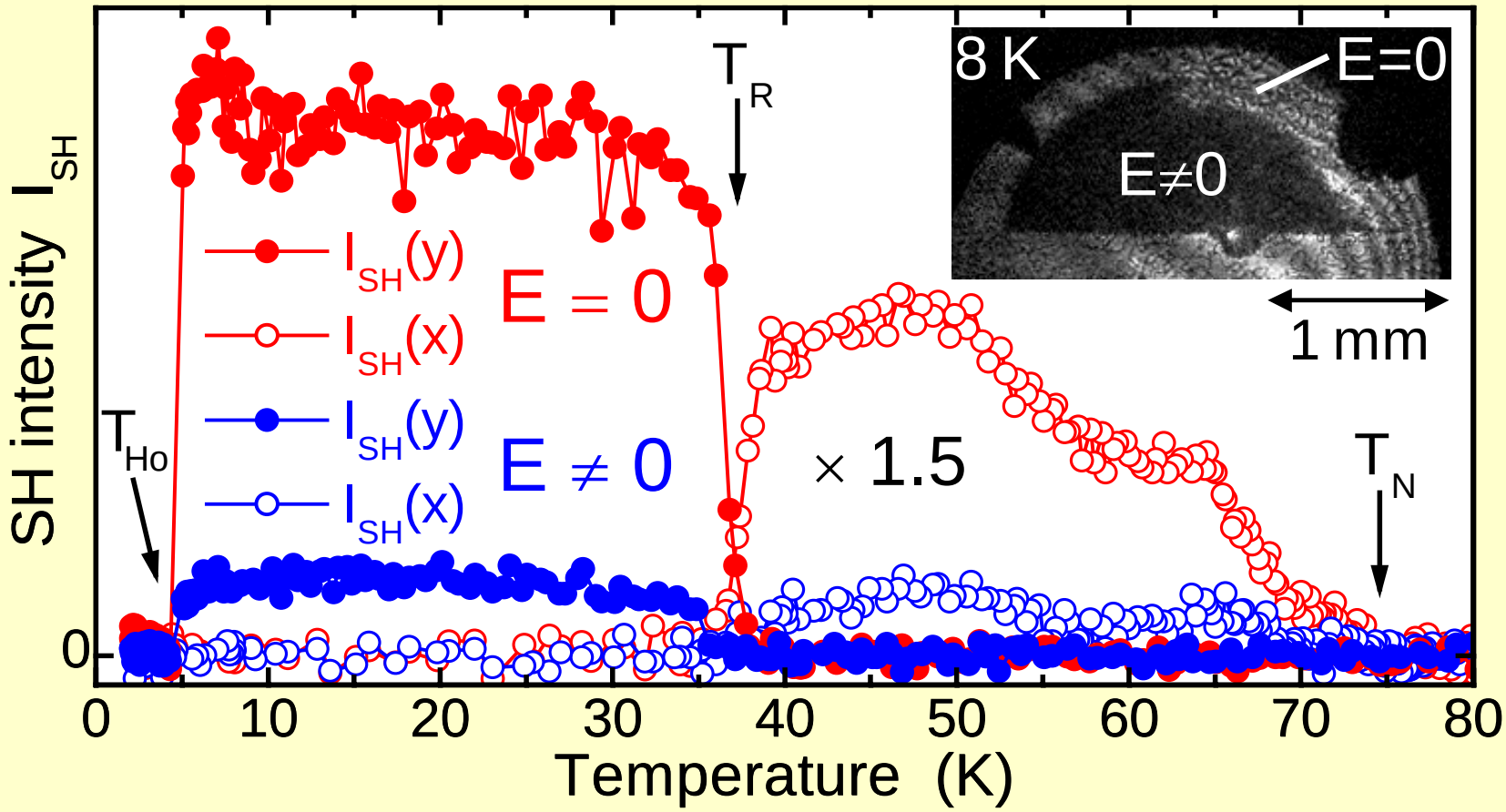

Electric field E changes magnetic structure right below $T_N = 75$ K

Magnetic Phase Control by Electric Field in $HoMnO_3$

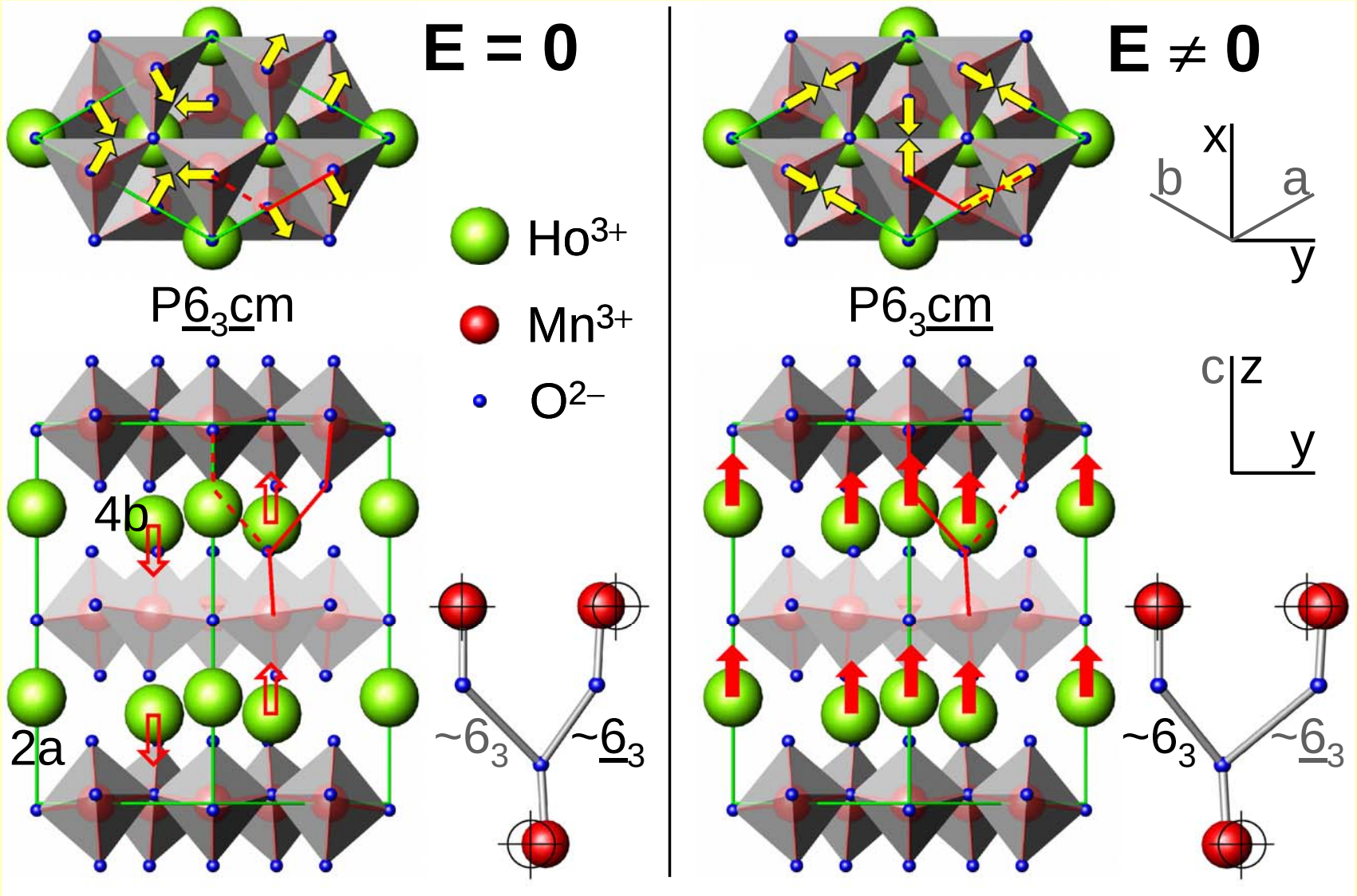

Nature **430**, 541 (2004)

SHG in Multiferroic Compounds

Two-dimensional expansion of the SH susceptibility χ for electric and magnetic order parameters

$$\vec{P}^{NL}(2\omega) = \varepsilon_0 \left[\hat{\chi}(0) + \hat{\chi}(\wp) + \hat{\chi}(\ell) + \hat{\chi}(\wp\,\ell) + \ldots\right] \vec{E}(\omega)\vec{E}(\omega)$$

$\chi(0)$:	Paraelectric paramagnetic contribution	——	always allowed
$\chi(P)$:	(Anti)ferroelectric contribution	⎫	allowed below
$\chi(\ell)$:	(Anti)ferromagnetic contribution	⎬	the respective
$\chi(P\ell)$:	Magnetoelectric contribution	⎭	ordering temperature

- SHG allows simultaneous investigation of magnetic and electric structures
- Selective access to electric and magnetic sublattices
- Magnetoelectric contribution reveals the interaction between the magnetic and electric sublattices in this ferroelectromagnet

Magnetoelectric Second Harmonic Generation

Source term	$S^{ED}(0)$	$S^{ED}(\mathcal{P})$	$S^{MD,EQ}(\ell)$	$S^{ED}(\mathcal{P}\ell)$
Sublattice sym.	$P6_3/mcm$	$P6_3cm$	$P6_3/\underline{m}c\underline{m}$	$P\underline{6_3}c\underline{m}$
SHG for $k \parallel z$	$= 0$	$= 0$	$\neq 0$	$\neq 0$
SHG for $k \parallel x$	$= 0$	$\neq 0$	$= 0$	

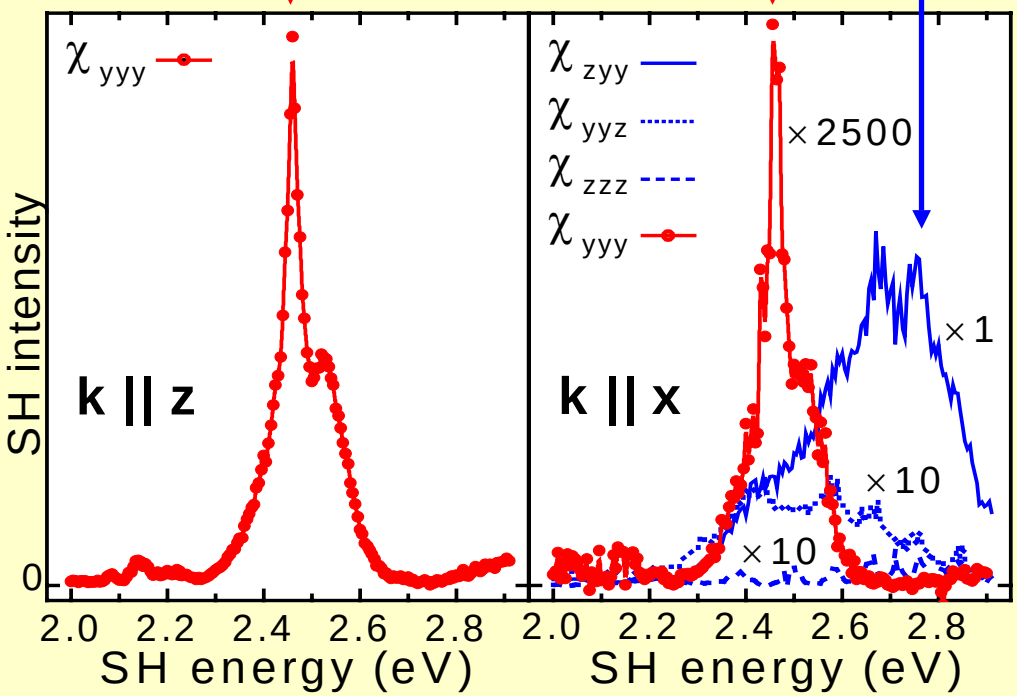

Identical magnetic spectra for k||z and k||x indicate **bilinear coupling to $\mathcal{P}$, ℓ.**

Unarbitrary evidence for the first observation of **"magnetoelectric SHG"**

Nature **419**, 818 (2002)

Coupling between Electric and Magnetic Domains

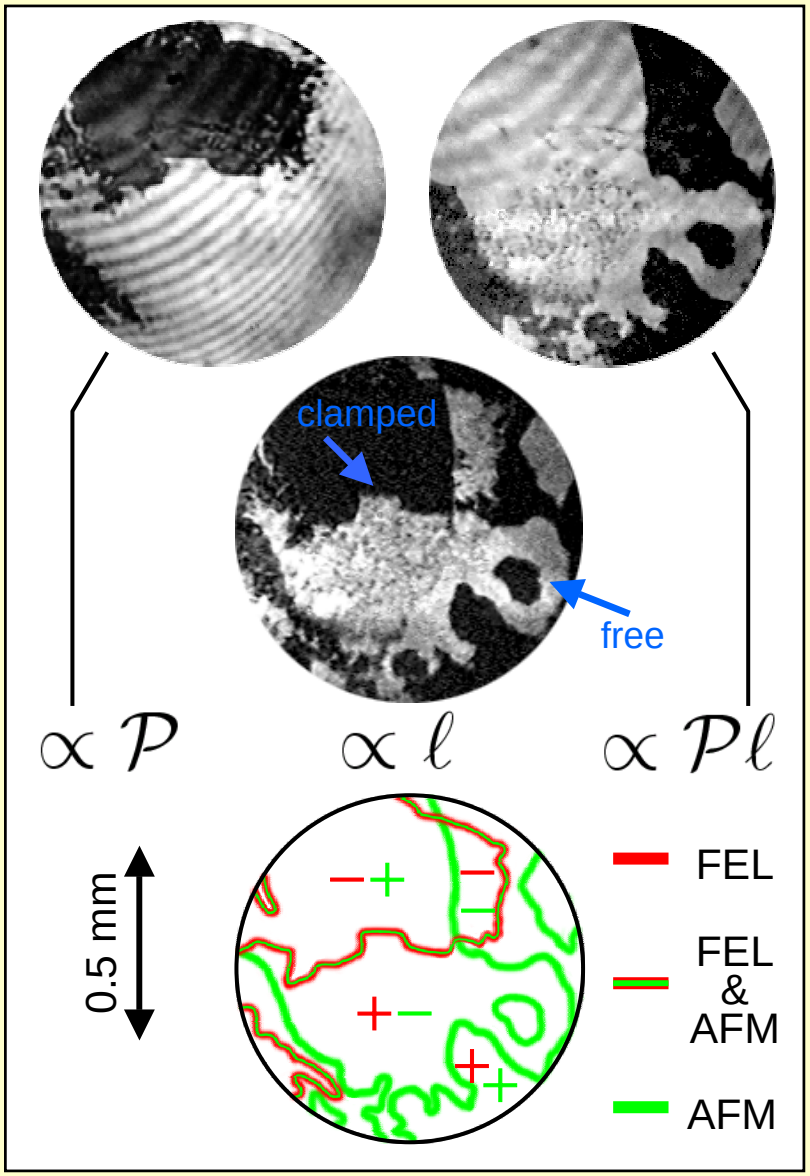

Coexisting domains in $YMnO_3$:

✧ Ferroelectric domains: $\propto \boldsymbol{P}$

✧ Antiferromagnetic domains: $\propto \ell$

✧ "Magneto-electric" domains: $\propto \boldsymbol{P}\ell$

$\boldsymbol{P}\ell = +1$ for $\boldsymbol{P} = \pm 1$, $\ell = \pm 1$
$\boldsymbol{P}\ell = -1$ for $\boldsymbol{P} = \pm 1$, $\ell = \mp 1$

➢ Any reversal of the FEL order parameter is clamped to a reversal of the AFM order parameter

➢ Coexistence of "free" and "clamped" AFM walls

Nature **419**, 818 (2002)

Magnetoelectric Interaction of Domain Walls

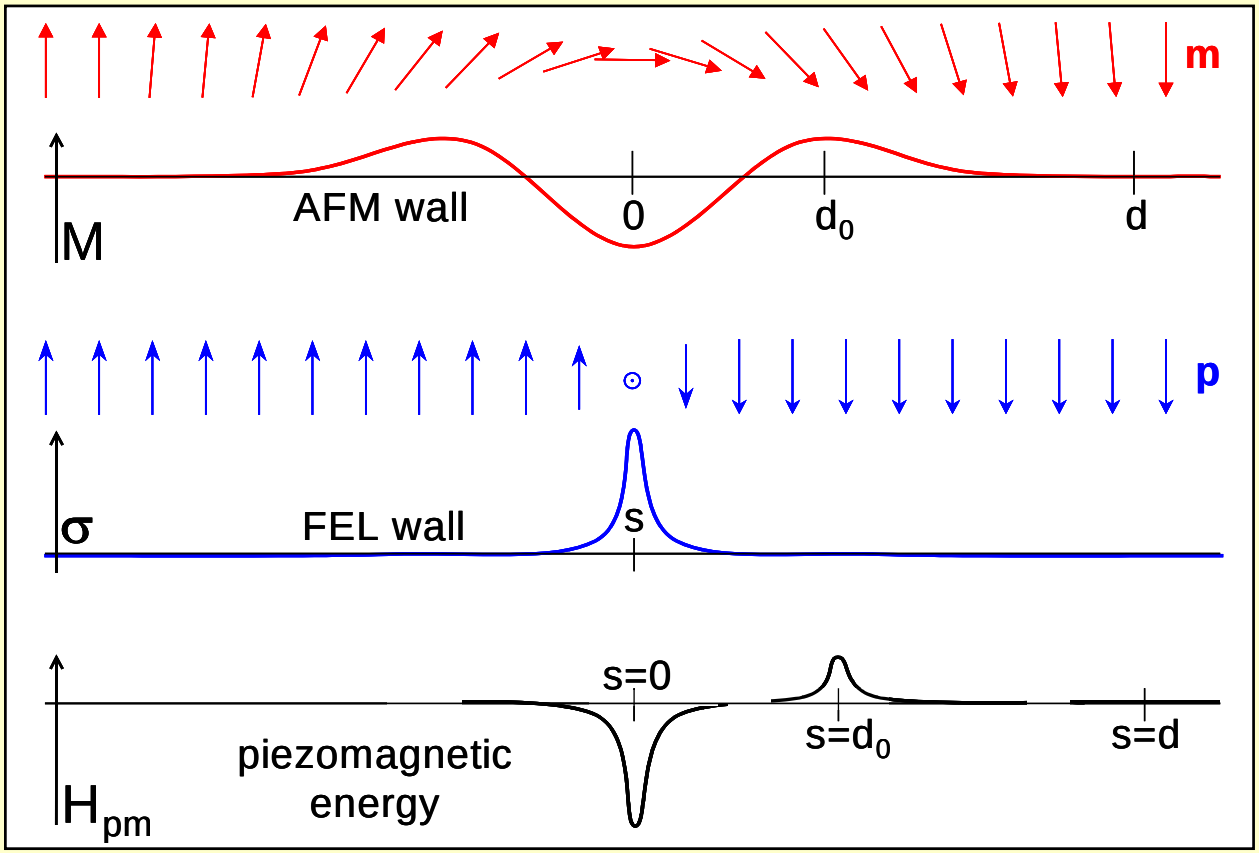

- AFM wall carries an intrinsic macroscopic mag-netization
- FEL wall induces strain due to switching of polarization
- Width of walls:
  - AFM – O[10^3] unit cells: small in-plane anisotropy
  - FEL – O[10^0] unit cells: large uniaxial anisotropy

Piezomagnetic contribution $H_{pm} = q_{ijk} M_i \sigma_{jk}$ with $\sigma \propto P_z$
$\rightarrow$ higher-order magnetoelectric effect

Generation of an antiferromagnetic wall clamped to a ferroelectric wall leads to reduction of free energy.

Phys. Rev. Lett. **90**, 177204 (2003)

Magnetoelectric Correlations in Multiferroics

- Nonlinear Optics and Symmetry
- Cr_2O_3 as Case Study
- Experimental Setup
- Magnetoelectric Effects in Multiferroic $RMnO_3$
- Summary

Summary

- Nonlinear optics as powerful probe for magnetic *and* electric structures as well as their magnetoelectric interaction
- Highly selective; direct access to ordered sub-lattices via symmetry principles
- Access to "additional degrees of freedom" of optical experiments
  - Spectroscopy (sub-lattice sensitivity, interacting sub-lattices)
  - Topography (*local* magnetic and electric structure, domains)
  - Time resolution (spin dynamics, ultrafast magnetic switching)
- Review: M. Fiebig et al., J. Opt. Soc. Amer. B **22**, 96 (2005)

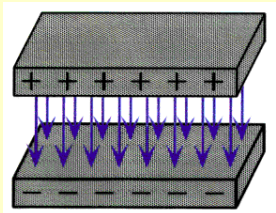

Spin electronics

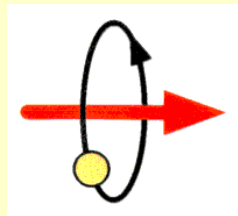

Semiconductor
e.g. GaAs

Magnetically doped semiconductor
e.g. $Cd_{1-x}Mn_xTe$

Magnetic crystals
e.g. NiO